Rapid and reliable thickness identification of two-dimensional nanosheets using optical microscopy**

Hai Li,[1,†] Jumiati Wu,[1,†] Xiao Huang,[1] Gang Lu,[1] Jian Yang,[1] Xin Lu,[2] Qihua Xiong,[2] Hua Zhang[1,]*

[1]School of Materials Science and Engineering, Nanyang Technological University, 50 Nanyang Avenue, Singapore 639798, Singapore

[2]Division of Physics and Applied Physics, School of Physical and Mathematical Sciences, Nanyang Technological University, 21 Nanyang Link, Singapore 637371, Singapore

*To whom correspondence should be addressed.

Phone: +65-6790-5175. Fax: +65-6790-9081

E-mail: hzhang@ntu.edu.sg

Website: http://www.ntu.edu.sg/home/hzhang/

[†]These authors contributed equally to this work.

ABSTRACT. The physical and electronic properties of ultrathin two-dimensional (2D) layered nanomaterials are highly related to their thickness. Therefore, the rapid and accurate identification of single- and few- to multi-layer nanosheets is essential to their fundamental study and practical applications. Here, a universal optical method has been developed for simple, rapid and reliable identification of single- to quindecuple-layer (1L-15L) 2D nanosheets, including graphene, MoS_2, WSe_2 and TaS_2, on Si substrates coated with 90 nm or 300 nm SiO_2. The optical contrast differences between the substrates and 2D nanosheets with different layer numbers were collected and tabulated, serving as a standard reference, from which the layer number of a given nanosheet can be readily and reliably determined without using complex calculation nor expensive instrument. Our general optical identification method will facilitate the thickness-dependent study of various 2D nanomaterials, and expedite their research toward practical applications.

KEYWORDS: Thickness identification, optical microscopy, 2D nanosheets, graphene, MoS_2, WSe_2, contrast difference

Two-dimensional (2D) layered nanomaterials, such as graphene and transition metal dichalcogenides (TMDs, e.g. MoS_2, $MoSe_2$, WS_2, WSe_2, $NbSe_2$, TiS_2, and TaS_2),[1-10] have attracted much attention in recent years due to their novel optical, electronic, mechanical and magnetic properties in contrast to their bulk crystals. Currently, mechanical exfoliation is still one of the most efficient ways to obtain high-quality, atomically thin nanosheets of 2D layered nanomaterials.[1, 3-7] However, this technique produces not only single- and few- to multi-layer nanosheets, but also a large quantity of thicker flakes. It is well known that the physical and electronic properties of 2D nanomaterials are highly related to their thickness.[3-6, 11-17] For example, while single-layer (1L) graphene is a zero–band gap semimetal, double-layer (2L) graphene is semiconducting with tunable band gap, leading to much higher on/off current ratios in field-effect transistors (FETs).[12, 18] Few-layer graphene also shows different energy band structures from 1L graphene, and exhibits some favorable optical and electronic properties for practical applications.[12-13, 18] Similar to graphene, TMD nanosheets also show the thickness-dependent band structures. For example, the 1L and 2L MoS_2 nanosheets with band gap of 1.82 eV and 1.65 eV, respectively, are attractive for green light detection, while triple-layer (3L) MoS_2 nanosheet with a band gap of 1.32 eV is more sensitive to red light.[16] On the other hand, multilayer MoS_2 nanosheets are attractive for fabrication of flexible transparent devices, due to their ease of fabrication, good mechanical and electronic stability, and ability to provide high current drive in the devices.[14, 19] Therefore, the rapid determination of location and layer number of mechanically exfoliated single- and few- to multi-layer nanosheets among copious thick flakes over a centimeter-/millimeter-size area is the first priority in their fundamental research and practical applications.

To date, many methods have been developed to identify the thickness of 2D nanosheets, such as atomic force microscopy (AFM), Raman spectroscopy and optical microscopy (OM). Although AFM is commonly used to measure the thickness of 2D nanosheets, it is time-consuming and not suitable for rapid measurement over large area. In addition, AFM measurement might be affected by the absorbed water layer under 2D nanosheets or instrumental offset.[20-21] As a result, the thickness of single-layer graphene measured by AFM varied from 0.4 to 0.9 nm.[18, 21-22] Raman spectroscopy is a quick characterization method to identify single- to few-layer 2D nanosheets.[12, 17, 23-25] However, the difference between double- and few-layer graphene or TMDs nanosheets in Raman spectra is insufficient to accurately distinguish them.[4, 23-24] Although low-frequency Raman spectroscopy (< 50 cm^{-1}) has been used to reliably determine the layer number of graphene, MoS_2 or WSe_2,[12, 17, 25] it requires expensive and nonstandard equipment. On the contrary, OM is a simple, efficient and nondestructive technique that enables rapid characterization of 2D nanosheets over large area.[4, 13, 20, 26-35] The OM method mainly relies on the optical contrast between a 2D nanosheet and the substrate for fast and unambiguous identification. To improve such contrast, several methods have been developed, including the use of narrow band illumination,[28, 36] selection of optimal substrate,[26, 30, 36] collection of reflection spectra,[20] measurement of total color difference[30] or ratio of color difference[29] *etc*. Unfortunately, these methods either involve special experimental setup or time-consuming image processing, and more importantly, they are not generalizable for identification of various kinds of nanosheets.

Here, we demonstrate a simple, rapid and reliable method to identify 2D nanosheets (*e.g.* graphene, MoS_2, WSe_2 and TaS_2) from single- to quindecuple-layer (1L-15L) without

using expensive instrument nor complex calculation. The contrast difference between the 2D nanosheet and substrate can be simply obtained from the brightness profile of their color images or grayscale images of R, G or B channel. The obtained values of contrast difference for nanosheets with different layer numbers can be plotted as a standard chart, based on which the layer number of a given nanosheet can be rapidly and accurately determined on Si substrate coated with 90 nm or 300 nm SiO_2, referred to 90 nm or 300 nm SiO_2/Si, respectively.

RESULTS AND DISCUSSION

Description of the optical identification method

The key to the reliable and accurate optical identification of a 2D nanosheet is to correlate its layer number with its optical contrast with respect to the substrate. In our method, the optical contrast of a nanosheet (defined as C) and substrate (defined as Cs) were directly measured from its color optical image by using a free software (ImageJ). The contrast difference (defined as C_D) is obtained by subtracting C with Cs (Equation 1). Similarly, for the grayscale image (from R, G or B channel), the contrast difference between the nanosheet and substrate (C_{DR}, C_{DG} or C_{DB}) is calculated by subtracting the contrast of the nanosheet (C_R, C_G or C_B) with that of the substrate (C_{SR}, C_{SG} or C_{SB}) (Equation 2-4).

$$C_D = C - C_S \quad (1)$$

$$C_{DR} = C_R - C_{SR} \quad (2)$$

$$C_{DG} = C_G - C_{SG} \quad (3)$$

$$C_{DB} = C_B - C_{SB} \quad (4)$$

As a demonstration, Figure 1a shows the color optical image of a MoS_2 flake on 90 nm SiO_2/Si. Fig. 1b is the contrast profile of the dashed rectangle highlighted in Figure 1a generated by ImageJ. The contrast values (C) of the octuple-layer (8L) and hextuple-layer (6L) MoS_2 nanosheets are 162.3 and 118.6, respectively, while the contrast value of 90 nm SiO_2/Si (C_S) is 120.4. According to equation (1), the contrast difference between the 8L (or 6L) MoS_2 nanosheet and 90 nm SiO_2/Si substrate is calculated to be C_D = 162.3 - 120.4 = 41.9 (or 118.6 -120.4 = -1.8).

Optical identification of 1L-15L graphene nanosheets on 90 nm SiO_2/Si

It has been reported that the color of a graphene nanosheet can be used to identify its thickness in combination with theoretical calculation.[30, 34] Theoretical calculation predicted that SiO_2 film with thickness of 90 or 300 nm is the optimal dielectric layer for optical identification of graphene.[13, 26, 35] Here, thickness identification of 1L-15L graphene nanosheets on 90 or 300 nm SiO_2/Si can be achieved by our simple, rapid and reliable method based on the measurement of optical contrast difference. Color optical images (Figure 2a-n), AFM measurement (Figure 2q) and Raman characterization (Supplementary Figure S1) were first used to locate exfoliated graphene nanosheets on 90 nm SiO_2/Si and determine their thicknesses. After that, optical contrast differences (C_D) between 1L-15L graphene nanosheets and 90 nm SiO_2/Si were measured from their color optical images taken at different exposure times by using ImageJ (Figure 2o). It can be seen that, for 1L-15L graphene nanosheets, the absolute value of C_D increases with increasing exposure time from 20 to 140 ms, and decreases from 160 to 300 ms. At 200 ms, as compared to other exposure times, such as 80 ms, the C_D values are mostly

distinguishable among the 1L-15L nanosheets (Figure 2p and Supplementary Table S1), especially for those thicker than 10L. Therefore, a standard chart of C_D values at 200 ms for different layer numbers was generated (Figure 2p and Supplementary Table S1), from which the thickness of a graphene nanosheet on 90 nm SiO_2/Si can be readily determined.

Similar to the C_D values, the C_{DR}, C_{DG} and C_{DB} values of 1L-15L graphene nanosheets on 90 nm SiO_2/Si, measured from grayscale images of R, G and B channels, respectively, can also be used for the layer number identification (Supplementary Figure S2 and Table S1). Similarly, the C_D, C_{DR} and C_{DG} values of 1L-13L graphene nanosheets on 300 nm SiO_2/Si can also be determined in the same manner and thus used for layer number identification of graphene (Supplementary Figures S3-S4).

Optical identification of 1L-15L MoS_2 nanosheets on 90 nm SiO_2/Si

As for the 1L-15L MoS_2 nanosheets on 90 nm SiO_2/Si (Figure 3a-n), they also show the thickness-dependent contrast difference at various exposure times (Figure 3o-p), confirmed by AFM measurement and low-frequency Raman characterization (Figure 3q and Supplementary Figure S5). It is shown that at the exposure time of 80 ms, 5L-15L MoS_2 nanosheets are distinguishable based on C_D values (Figure 3o-p and Supplementary Table S2). However, the C_D values of 1L-4L MoS_2 nanosheets are less differentiable, and especially the C_D values of 2L and 3L nanosheets are close, ~ -55 (Figure 3p and Figure 4 a-b). In order to effectively distinguish 1L-4L MoS_2 nanosheets on 90 nm SiO_2/Si, the optical contrast differences measured from their grayscale images from R, G and B channels (C_{DR}, C_{DG} and C_{DB}) were used to determine their thicknesses (Figure 4c-i). As shown in Figure 4g-i, the C_{DB} values of 1L and 2L MoS_2 nanosheets are negative (1L: -

26.4; 2L: -15.4), while those of 3L and 4L MoS_2 nanosheets are positive (3L: 4.2; 4L: 28.5). Meanwhile, the C_{DR} and C_{DG} values of 1L-4L MoS_2 nanosheets are also discrete enough for their thickness identification (Figure 4d, f and i). Therefore, 1L-15L MoS_2 nanosheets on 90 nm SiO_2/Si can be easily identified based on the measured C_D, C_{DR}, C_{DG} and C_{DB} values.

An interesting feature was observed in the plot of C_D (or C_{DR}, C_{DG} and C_{DB}) vs. layer number of MoS_2. For example, there is a transition of C_D value between 5L and 6L nanosheets (Figure 3p and Supplementary Table S2) from negative C_D at 5L (-21.8 ± 0.5) to positive C_D at 6L (1.0 ± 0.7). In other words, compared to the 90 nm SiO_2/Si substrate, 1L-5L MoS_2 nanosheets are darker while 6L-15L MoS_2 nanosheets are brighter under white light illumination. In this work, the thickness of a nanosheet with a minimum positive C_D value (similar for C_{DR}, C_{DG} or C_{DB}) is defined as the transitional thickness (T_C). In this case, the T_C for MoS_2 nanosheets in color image, grayscale image from R, G or B channel is 6L, 10L, 5L and 3L, respectively (Table 1). Therefore, the sign (positive or negative) of the C_D value enables the fast determination of the thickness range of a nanosheet (i.e. below T_C or above T_C).

Similar to MoS_2 nanosheets on 90 nm SiO_2/Si, 1L-15L MoS_2 nanosheets on 300 nm SiO_2/Si can also be reliably identified by measuring the C_D value in combination with the C_{DR}, C_{DG} and C_{DB} values (Supplementary Figure S6 and Table S2).

Optical identification of single- to quattuordecuple-layer (1L-14L) WSe_2 nanosheets on 90 nm SiO_2/Si

The optical contrast difference can also be used to identify 1L-14L WSe_2 nanosheets on 90 or 300 nm SiO_2/Si. Figure 5a-l show the color optical images of 1L-14L WSe_2 nanosheets on 90 nm SiO_2/Si taken at the exposure time of 80 ms. The thickness of these nanosheets were confirmed by AFM measurement and low-frequency Raman spectra (Figure 5o and Supplementary Figure S7). As shown in Figure 5m, the C_D values are distinguishable for 6L-14L WSe_2 nanosheets, but are difficult to be differentiated for 1L-5L nanosheets. As shown in Figure 5m and Supplementary Table S3, the 2L-4L WSe_2 nanosheets have similar C_D values (2L: -59.2 ± 1.4; 3L: -62.9 ± 1.5; 4L: -55.3 ± 1.4), so do 1L and 5L WSe_2 nanosheets (1L: -38.4 ± 1.7; 5L: -36.8 ± 2.4). In this case, the grayscale images of R, G and B channels were used to indicate the difference among the 1L-5L WSe_2 nanosheets (Figure 5n). By comparing C_{DR}, C_{DG} and C_{DB} values at various layer numbers, it was found that the C_{DR} values combined with C_{DB} values are mostly suitable to rapidly differentiate 1L-5L WSe_2 nanosheets because of the sufficient gap between the C_{DR} and C_{DB} values of adjacent layer numbers (Supplementary Table S3). The C_{DB} value of 1L WSe_2 nanosheet is negative (-27.6 ± 1.4) while that of 5L WSe_2 nanosheet is positive (16.7 ± 0.9). In addition, the T_C of C_{DB} values is 4L WSe_2 nanosheet (0.3 ± 0.8). Thus 1L, 4L and 5L WSe_2 nanosheets can be easily identified by reading the C_{DB} values. Although 2L and 3L WSe_2 nanosheets have similar C_{DG} values (2L: -76.8 ± 1.4; 3L: -76.5 ± 1.9), their C_{DR} values (2L: -80.0 ± 0.9; 3L: -103.0 ± 0.4) are fairly discrete for thickness identification. Thus, 1L-14L WSe_2 nanosheets on 90 nm SiO_2/Si can be readily identified using the C_D values in combination with C_{DR} and C_{DB} values. Furthermore, for 1L-14L WSe_2 nanosheets on 300 nm SiO_2/Si, their C_D, C_{DR}, C_{DG} and C_{DB} values are also distinguishable for fast thickness determination (Supplementary

Figure S8 and Table S3).

Verification of layer number identification of MoS_2 and WSe_2 nanosheets on 90 nm SiO_2/Si

In order to verify the accuracy of our optical method, the thicknesses of mechanically exfoliated graphene, MoS_2 and WSe_2 nanosheets on 90 nm SiO_2/Si were firstly identified using the measurement of C_D values followed by AFM measurement to confirm it.

Taking graphene as an example, Figure 6a shows the color optical image of a graphene nanosheet. As shown in Figure 6b, the C_D values measured from the red dashed rectangle shown in Figure 6a are -10.7, -57.6 and -68.3, respectively. According to the standard chart shown in Figure 2o-p and Supplementary Table S1, these C_D values correspond to 1L, 5L and 6L graphene nanosheets, respectively. AFM measurement on these regions show thicknesses of 0.4, 1.7 and 2.1 nm (Figure 6c-d), respectively, consistent with the thickness of 1L, 5L and 6L graphene (Figure 2q and Table S5 in SI), respectively, confirming the accuracy of the optical identification result.

As for MoS_2, Figure 7a shows the color optical image of an exfoliated MoS_2 nanosheet, displaying three distinct color regions. C_D values measured from the red dashed rectangle shown in Figure 7a are -2.5, 22.4 and 60.3, respectively, which correspond to 6L, 7L and 9L MoS_2 nanosheets according to the standard chart shown in Figure 3o-p and Supplementary Table S2. The corresponding thickness of the these three regions measured by AFM (Figure 7c-d) are 4.1, 4.7 and 5.9 nm, respectively, consistent with that of 6L, 7L and 9L MoS_2 nanosheets.

Similarly, for the optical identification of WSe_2 nanosheets, C_D values of 9.5 and 30.8

(Figure 7f) were first obtained from two different color regions (highlighted in the red dashed rectangle shown in Figure 7e), corresponding to 7L and 8L WSe_2 nanosheets, respectively, by referring to the standard chart shown in Figure 5m and Supplementary Table S3. AFM measurement (Figure 7g-h) on these two regions indicates thicknesses of 4.7 and 5.4 nm, respectively, in agreement with that of 7L and 8L WSe_2 nanosheets (Figure 5o and Supplementary Table S5).

Besides graphene, MoS_2 and WSe_2 nanosheets, our method can also be used for the rapid and reliable identification of TaS_2 nanosheets on 90 nm SiO_2/Si. The C_D values of 2L-8L, 15L to octoviguple-layer (28L) and duotriguple-layer (32L) TaS_2 nanosheets are discrete enough for reliable identification (Supplementary Figure S9 and Table S4). In combination with the C_{DR}, C_{DG} and C_{DB} values (Supplementary Table S4), 2L-28L and 32L TaS_2 nanosheets can be easily and reliably identified (Supplementary Figures S9-S10), indicating the generalizability of our method in the thickness identification of 2D nanosheets.

The measurement of C_D is affected by the intensity of illumination, thickness of SiO_2 film, and exposure time. In our work, the thickness of SiO_2 film and exposure time are fixed. Therefore, the measurement error (characterized by the standard deviation, SD) likely arises from the fluctuation of illumination intensity, which is manually adjusted in our optical microscope (Supplementary Figure S11). Nevertheless, the measurement error is much smaller than the difference between C_D values of adjacent layers. In other words, the difference among C_D values is sufficient for thickness determination. In addition, the transition thickness (T_C) of optical contrast difference is related to the type of material, the thickness of SiO_2 film, as well as the color of optical image. As shown in Table 1, the

T_C values of C_D, C_{DR}, C_{DG} and C_{DB} follow the order of $C_{DR} > C_D \geq C_{DG} > C_{DB}$ for 1L-15L MoS_2 and 1L-14L WSe_2 nanosheets on 90 and 300 nm SiO_2/Si. In the case of TaS_2 nanosheets on 90 nm SiO_2/Si, the T_C values of C_D, C_{DR} and C_{DG} follow the order of $C_D > C_{DG} > C_{DR}$ (Table 1). In terms of graphene nanosheets on 90 and 300 nm SiO_2/Si, the T_C values of C_D, C_{DR}, C_{DG} and C_{DB} are much larger compared to those of MoS_2, WSe_2 and TaS_2 nanosheets (Table 1 and Supplementary Figures S12-13). The variation of T_C for different materials might be attributed to their intrinsic properties, such as refractive index.

CONCLUSION

In summary, a universal optical method has been developed for simple, rapid and reliable identification of 1L-15L 2D nanosheets, including graphene, MoS_2, WSe_2 and TaS_2, on 90 and 300 nm SiO_2/Si. By processing the color optical images and the grayscale images of R, G and B channels, the optical contrast differences between 2D nanosheets and SiO_2/Si were measured using ImageJ and plotted as standard charts to guide the layer number identification. The transition of C_D, C_{DR}, C_{DG}, and C_{DB} values can be used as clear mark for quick identification of layer number. Neither complex calculation nor special instrument is required in our method, making it applicable for any labs equipped with standard optical microscope and digital camera. Our simple optical identification method will facilitate the fundamental study and practical applications of 2D nanomaterials, and accelerate their progress towards future commercialization. Furthermore, our method potentially expands the capability of optical microscope in study of nanomaterials and applications of nanotechnology.

METHODS AND MATERIALS

Mechanical exfoliation of 2D nanosheets (graphene, MoS_2, WSe_2 and TaS_2 nanosheets). Natural graphite (NGS Naturgraphit GmbH, Germany), MoS_2 crystals (SPI Supplies, USA), WSe_2 and TaS_2 crystals (Nanoscience Instruments, Inc., USA) were used for preparation of mechanically-exfoliated 2D nanosheets, respectively, which then were deposited onto the freshly cleaned 90 and 300 nm SiO_2-coated Si substrates (90 and 300 nm SiO_2/Si).

Capture of optical images of 2D nanosheets. The bright-field optical microscope (Eclipse LV100D with a 100×, 0.9 numerical aperture (NA) objective, Nikon) was used to locate and image the 2D nanosheets. A lamphouse (LV-LH50PC) equipped with high-intensity halogen lamp (12V-50W) was used as light source. The intensity of light source was adjusted by turning the brightness control knob to level 9 (Supplementary Figure S11). For graphene and MoS_2 nanosheets on 90 nm SiO_2/Si, the optical images were captured at the exposure time of 20, 40, 60, 80, 100, 120, 140, 160, 180, 200, 250 and 300 ms, respectively. For WSe_2 and TaS_2 nanosheets on 90 nm SiO_2/Si, the optical images were captured at the exposure time of 80 ms. For various 2D nanosheets on 300 nm SiO_2/Si, the optical images were captured at the exposure time of 50 ms. A DS camera head (DS-Fi1) with a digital camera control unit (DS-U3) was used to capture color optical images of 2D nanosheets at the resolution of 1280 × 960 pixels. The imaging software is NIS-Elements F (version 4.00.06) and the white balance is calibrated as R/B=1.23:1.24 (Supplementary Figure S11). In order to give quantitative and statistic characterization of the layer numbers of 2D nanosheets, a large amount of graphene,

MoS_2, WSe_2 and TaS_2 flakes with layer numbers ranged from 1L to 32L, prepared by the mechanical cleavage technique, was imaged by optical microscopy and analyzed by using our optical method. For 1L to 10L 2D nanosheets, at least 5 samples were collected for measurement. For 2D nanosheets thicker than 11L, usually 3 samples were collected for measurement.

Optical contrast difference measurement of color optical images and grayscale images of R, G and B channels by using ImageJ. The color optical images of 2D nanosheets were processed by the ImageJ (version 1.46p, National Institutes of Health, USA). For the color image (RGB image), the contrast value of each pixel (C_V), i.e. brightness value, is calculated using the following equation,

$$C_V = (C_{VR} + C_{VG} + C_{VB})/3 \quad (5)$$

where, C_{VR}, C_{VG} and C_{VB} are the R, G and B values per pixel in color image, respectively. 0 means darkest and 255 means brightest.

The grayscale images of R, G and B channels were extracted by using the "Split Channels" command from "Image > Color > Split Channels" in the menu bar, where 0 means darkest and 255 means brightest. In the grayscale image, we can drag the left button of mouse to draw a rectangular box across the 2D nanosheet and then press "K" to obtain the contrast profile of the selected area. In the plot of contrast profile, click "List" to show the contrast values of the 2D nanosheet and SiO_2 substrate.

The detailed optical contrast difference (C_D, C_{DR}, C_{DG} and C_{DB}) values of 2D nanosheets are listed in Supplementary Table S1-S4.

Thickness measurement of 2D nanosheets by AFM. AFM (Dimension ICON with NanoScope V controller, Bruker, USA) was used to confirm the layer number of 2D

nanosheets by measuring the film thickness in tapping mode in air. The thickness values of 2D nanosheets are listed in Supplementary Table S5.

Raman measurement of 2D nanosheets. Analysis of the MoS_2 and WSe_2 nanosheets by low-frequency Raman spectroscopy was carried out at room temperature using a micro-Raman spectrometer (Horiba-JY T64000) equipped with a liquid nitrogen cooled charge-coupled device. The measurements were conducted in a backscattering configuration excited with a solid state green laser (λ = 532 nm). A reflecting Bragg grating (OptiCrate) followed by another ruled reflecting grating was used to filter the laser side bands, as such ~8 cm^{-1} limit of detection was achieved using most solid state or gas laser lines. All spectra were collected through a 100× objective and dispersed by a 1800 g/mm grating under a triple subtractive mode with a spectra resolution of 1 cm^{-1}. The Raman spectra were calibrated by using the peak of Si substrate (520 cm^{-1}). The laser power at the sample surface was less than 1.5 mW for MoS_2 and 0.3 mW for WSe_2, respectively.

Analysis of graphene nanosheets by Raman spectroscopy was carried out on a WITec CRM200 confocal Raman microscopy system with the excitation line of 488 nm and an air cooling charge coupled device (CCD) as the detector (WITec Instruments Corp, Germany).

Acknowledgement.

This work was supported by AcRF Tier 1 (RG 61/12) and Start-Up Grant (M4080865.070.706022) in Singapore. This research is also funded by the Singapore National Research Foundation and the publication is supported under the Campus for Research Excellence And Technological Enterprise (CREATE) programme.

Corresponding Author

*E-mail: hzhang@ntu.edu.sg, hzhang166@yahoo.com.

Phone: +65-6790-5175. Fax: +65-6790-9081

Website: http://www.ntu.edu.sg/home/hzhang/

Conflict of Interest: The authors declare no competing financial interest.

Supporting Information Available. Raman spectra of 1L-15L graphene, MoS_2 and WSe_2 nanosheets. Optical images and contrast difference plots of 1L-15L graphene, MoS_2 and WSe_2 nanosheets on 300 nm SiO_2/Si. Optical images and contrast difference plots of 2L-28L and 32L TaS_2 nanosheets on 90 nm SiO_2/Si. The detailed optical contrast difference (C_D, C_{DR}, C_{DG} and C_{DB}) and height values of 2D nanosheets. These materials are available free of charge *via* the Internet at http://pubs.acs.org.

REFERENCES AND NOTES

1. Chhowalla, M.; Shin, H. S.; Eda, G.; Li, L. J.; Loh, K. P.; Zhang, H., The Chemistry of Two-Dimensional Layered Transition Metal Dichalcogenide Nanosheets. *Nat. Chem.* **2013,** *5*, 263-275.
2. Huang, X.; Yin, Z. Y.; Wu, S. X.; Qi, X. Y.; He, Q. Y.; Zhang, Q. C.; Yan, Q. Y.; Boey, F.; Zhang, H., Graphene-Based Materials: Synthesis, Characterization, Properties, and Applications. *Small* **2011,** *7*, 1876-1902.
3. Li, H.; Lu, G.; Wang, Y.; Yin, Z. Y.; Cong, C.; He, Q.; Wang, L.; Ding, F.; Yu, T.; Zhang, H., Mechanical Exfoliation and Characterization of Single- and Few-Layer Nanosheets of WSe_2, TaS_2, and $TaSe_2$. *Small* **2013,** *9*, 1974-1981.
4. Li, H.; Lu, G.; Yin, Z. Y.; He, Q. Y.; Li, H.; Zhang, Q.; Zhang, H., Optical Identification of Single- and Few-Layer MoS_2 Sheets. *Small* **2012,** *8*, 682-686.
5. Li, H.; Yin, Z. Y.; He, Q. Y.; Li, H.; Huang, X.; Lu, G.; Fam, D. W. H.; Tok, A. I. Y.; Zhang, Q.; Zhang, H., Fabrication of Single- and Multilayer MoS_2 Film-Based Field-Effect Transistors for Sensing NO at Room Temperature. *Small* **2012,** *8*, 63-67.
6. Wang, Q. H.; Kalantar-Zadeh, K.; Kis, A.; Coleman, J. N.; Strano, M. S.,

Electronics and Optoelectronics of Two-Dimensional Transition Metal Dichalcogenides. *Nat. Nanotechnol.* **2012,** *7*, 699-712.
7. Yin, Z. Y.; Li, H.; Li, H.; Jiang, L.; Shi, Y. M.; Sun, Y. H.; Lu, G.; Zhang, Q.; Chen, X. D.; Zhang, H., Single-Layer MoS_2 Phototransistors. *ACS Nano* **2012,** *6*, 74-80.
8. Coleman, J. N.; Lotya, M.; O'Neill, A.; Bergin, S. D.; King, P. J.; Khan, U.; Young, K.; Gaucher, A.; De, S.; Smith, R. J.; Shvets, I. V.; Arora, S. K.; Stanton, G.; Kim, H. Y.; Lee, K.; Kim, G. T.; Duesberg, G. S.; Hallam, T.; Boland, J. J.; Wang, J. J.; Donegan, J. F.; Grunlan, J. C.; Moriarty, G.; Shmeliov, A.; Nicholls, R. J.; Perkins, J. M.; Grieveson, E. M.; Theuwissen, K.; McComb, D. W.; Nellist, P. D.; Nicolosi, V., Two-Dimensional Nanosheets Produced by Liquid Exfoliation of Layered Materials. *Science* **2011,** *331*, 568-571.
9. Radisavljevic, B.; Radenovic, A.; Brivio, J.; Giacometti, V.; Kis, A., Single-Layer MoS_2 Transistors. *Nat. Nanotechnol.* **2011,** *6*, 147-150.
10. Zeng, Z. Y.; Yin, Z. Y.; Huang, X.; Li, H.; He, Q. Y.; Lu, G.; Boey, F.; Zhang, H., Single-Layer Semiconducting Nanosheets: High-Yield Preparation and Device Fabrication. *Angew. Chem. Int. Ed.* **2011,** *50*, 11093-11097.
11. Li, H.; Qi, X. Y.; Wu, J.; Zeng, Z. Y.; Wei, J.; Zhang, H., Investigation of MoS_2 and Graphene Nanosheets by Magnetic Force Microscopy. *ACS Nano* **2013,** *7*, 2842-2849.
12. Tan, P. H.; Han, W. P.; Zhao, W. J.; Wu, Z. H.; Chang, K.; Wang, H.; Wang, Y. F.; Bonini, N.; Marzari, N.; Pugno, N.; Savini, G.; Lombardo, A.; Ferrari, A. C., The Shear Mode of Multilayer Graphene. *Nat. Mater.* **2012,** *11*, 294-300.
13. Nolen, C. M.; Denina, G.; Teweldebrhan, D.; Bhanu, B.; Balandin, A. A., High-Throughput Large-Area Automated Identification and Quality Control of Graphene and Few-Layer Graphene Films. *ACS Nano* **2011,** *5*, 914-922.
14. Kim, S.; Konar, A.; Hwang, W. S.; Lee, J. H.; Lee, J.; Yang, J.; Jung, C.; Kim, H.; Yoo, J. B.; Choi, J. Y.; Jin, Y. W.; Lee, S. Y.; Jena, D.; Choi, W.; Kim, K., High-Mobility and Low-Power Thin-Film Transistors Based on Multilayer MoS_2 Crystals. *Nat. Commun.* **2012,** *3*, 1011.
15. Das, S.; Chen, H. Y.; Penumatcha, A. V.; Appenzeller, J., High Performance Multilayer MoS_2 Transistors with Scandium Contacts. *Nano Lett.* **2013,** *13*, 100-105.
16. Lee, H. S.; Min, S. W.; Chang, Y. G.; Park, M. K.; Nam, T.; Kim, H.; Kim, J. H.; Ryu, S.; Im, S., MoS_2 Nanosheet Phototransistors with Thickness-Modulated Optical Energy Gap. *Nano Lett.* **2012,** *12*, 3695-3700.
17. Zhao, Y. Y.; Luo, X.; Li, H.; Zhang, J.; Araujo, P. T.; Gan, C. K.; Wu, J.; Zhang, H.; Quek, S. Y.; Dresselhaus, M. S.; Xiong, Q. H., Inter Layer Breathing and Shear Modes in Few-Trilayer MoS_2 and WSe_2. *Nano Lett.* **2013,** *13*, 1007-1015.
18. Koh, Y. K.; Bae, M. H.; Cahill, D. G.; Pop, E., Reliably Counting Atomic Planes of Few-Layer Graphene ($n > 4$). *ACS Nano* **2011,** *5*, 269-274.
19. Yoon, J.; Park, W.; Bae, G.-Y.; Kim, Y.; Jang, H. S.; Hyun, Y.; Lim, S. K.; Kahng, Y. H.; Hong, W.-K.; Lee, B. H.; Ko, H. C., Highly Flexible and Transparent Multilayer MoS_2 Transistors with Graphene Electrodes. *Small* **2013**, DOI:10.1002/smll.201300134.
20. Ni, Z. H.; Wang, H. M.; Kasim, J.; Fan, H. M.; Yu, T.; Wu, Y. H.; Feng, Y. P.; Shen, Z. X., Graphene Thickness Determination Using Reflection and Contrast Spectroscopy. *Nano Lett.* **2007,** *7*, 2758-2763.
21. Xu, K.; Cao, P. G.; Heath, J. R., Graphene Visualizes the First Water Adlayers on Mica at Ambient Conditions. *Science* **2010,** *329*, 1188-1191.

22. Cheng, Z. G.; Zhou, Q. Y.; Wang, C. X.; Li, Q. A.; Wang, C.; Fang, Y., Toward Intrinsic Graphene Surfaces: A Systematic Study on Thermal Annealing and Wet-Chemical Treatment of SiO_2-Supported Graphene Devices. *Nano Lett.* **2011,** *11*, 767-771.
23. Lee, C.; Yan, H.; Brus, L. E.; Heinz, T. F.; Hone, J.; Ryu, S., Anomalous Lattice Vibrations of Single- and Few-Layer MoS_2. *ACS Nano* **2010,** *4*, 2695-2700.
24. Hao, Y. F.; Wang, Y. Y.; Wang, L.; Ni, Z. H.; Wang, Z. Q.; Wang, R.; Koo, C. K.; Shen, Z. X.; Thong, J. T. L., Probing Layer Number and Stacking Order of Few-Layer Graphene by Raman Spectroscopy. *Small* **2010,** *6*, 195-200.
25. Zhang, X.; Han, W. P.; Wu, J. B.; Milana, S.; Lu, Y.; Li, Q. Q.; Ferrari, A. C.; Tan, P. H., Raman Spectroscopy of Shear and Layer Breathing Modes in Multilayer MoS_2. *Phys. Rev. B* **2013,** *87*, 115413.
26. Blake, P.; Hill, E. W.; Neto, A. H. C.; Novoselov, K. S.; Jiang, D.; Yang, R.; Booth, T. J.; Geim, A. K., Making Graphene Visible. *Appl. Phys. Lett.* **2007,** *91*, 063124.
27. Gaskell, P. E.; Skulason, H. S.; Rodenchuk, C.; Szkopek, T., Counting Graphene Layers on Glass via Optical Reflection Microscopy. *Appl. Phys. Lett.* **2009,** *94*, 143101.
28. Castellanos-Gomez, A.; Agrait, N.; Rubio-Bollinger, G., Optical Identification of Atomically Thin Dichalcogenide Crystals. *Appl. Phys. Lett.* **2010,** *96*, 213116.
29. Chen, Y. F.; Liu, D.; Wang, Z. G.; Li, P. J.; Hao, X.; Cheng, K.; Fu, Y.; Huang, L. X.; Liu, X. Z.; Zhang, W. L.; Li, Y. R., Rapid Determination of the Thickness of Graphene Using the Ratio of Color Difference. *J. Phys. Chem. C* **2011,** *115*, 6690-6693.
30. Gao, L. B.; Ren, W. C.; Li, F.; Cheng, H. M., Total Color Difference for Rapid and Accurate Identification of Graphene. *ACS Nano* **2008,** *2*, 1625-1633.
31. Wang, Y. Y.; Gao, R. X.; Ni, Z. H.; He, H.; Guo, S. P.; Yang, H. P.; Cong, C. X.; Yu, T., Thickness Identification of Two-Dimensional Materials by Optical Imaging. *Nanotechnology* **2012,** *23*, 495713.
32. Late, D. J.; Liu, B.; Matte, H. S. S. R.; Rao, C. N. R.; Dravid, V. P., Rapid Characterization of Ultrathin Layers of Chalcogenides on SiO_2/Si Substrates. *Adv. Funct. Mater.* **2012,** *22*, 1894-1905.
33. Jung, I.; Pelton, M.; Piner, R.; Dikin, D. A.; Stankovich, S.; Watcharotone, S.; Hausner, M.; Ruoff, R. S., Simple Approach for High-Contrast Optical Imaging and Characterization of Graphene-Based Sheets. *Nano Lett.* **2007,** *7*, 3569-3575.
34. Roddaro, S.; Pingue, P.; Piazza, V.; Pellegrini, V.; Beltram, F., The Optical Visibility of Graphene: Interference Colors of Ultrathin Graphite on SiO_2. *Nano Lett.* **2007,** *7*, 2707-2710.
35. Casiraghi, C.; Hartschuh, A.; Lidorikis, E.; Qian, H.; Harutyunyan, H.; Gokus, T.; Novoselov, K. S.; Ferrari, A. C., Rayleigh Imaging of Graphene and Graphene Layers. *Nano Lett.* **2007,** *7*, 2711-2717.
36. Benameur, M. M.; Radisavljevic, B.; Heron, J. S.; Sahoo, S.; Berger, H.; Kis, A., Visibility of Dichalcogenide Nanolayers. *Nanotechnology* **2011,** *22*, 125706.

Figure Caption

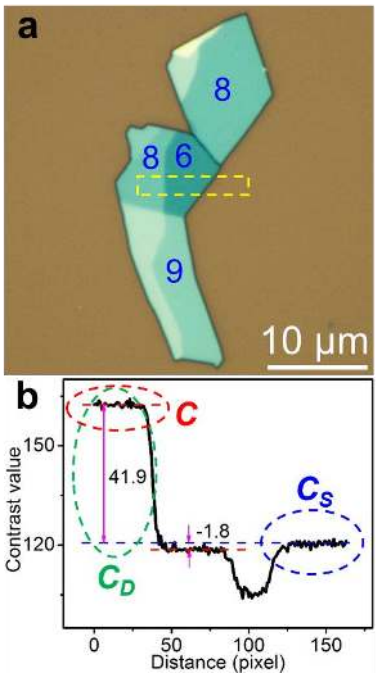

Figure 1. (a) Color optical image of a MoS_2 flake deposited on 90 nm SiO_2/Si. The digitals shown in (a) indicate the layer numbers of MoS_2 nanosheets. (b) Contrast profile of the dashed rectangle shown in (a). C_S: contrast of 90 nm SiO_2/Si. C: contrast of MoS_2 nanosheet. C_D: the contrast difference between MoS_2 nanosheet and 90 nm SiO_2/Si.

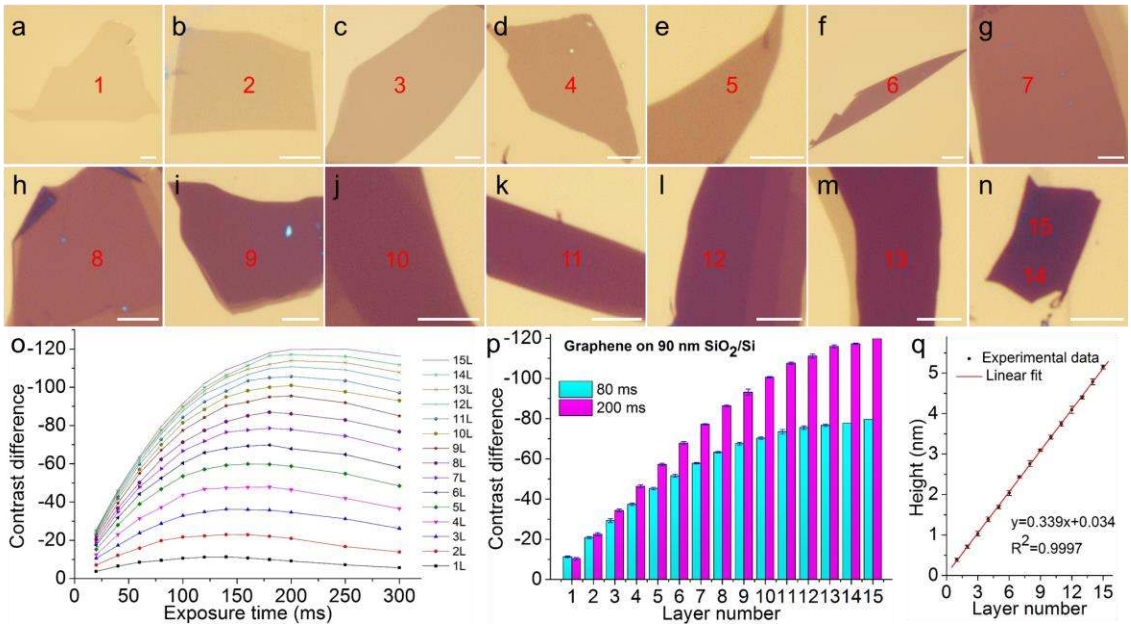

Figure 2. (a-n) Color optical images of 1L-15L graphene nanosheets on 90 nm SiO_2/Si. The scale bars shown in (a-n) are 10 μm. The digitals shown in (a-n) indicate the layer numbers of corresponding graphene nanosheets. (o) Plot of measured C_D values of 1L-15L graphene nanosheets on 90 nm SiO_2/Si at the exposure time of 20, 40, 60, 80, 100, 120, 140, 160, 180, 200, 250 and 300 ms, respectively. (p) Plot of measured C_D values of 1L-15L graphene nanosheets on 90 nm SiO_2/Si at the exposure time of 80 and 200 ms, respectively. (q) The thickness of 1L-15L graphene nanosheets measured by AFM.

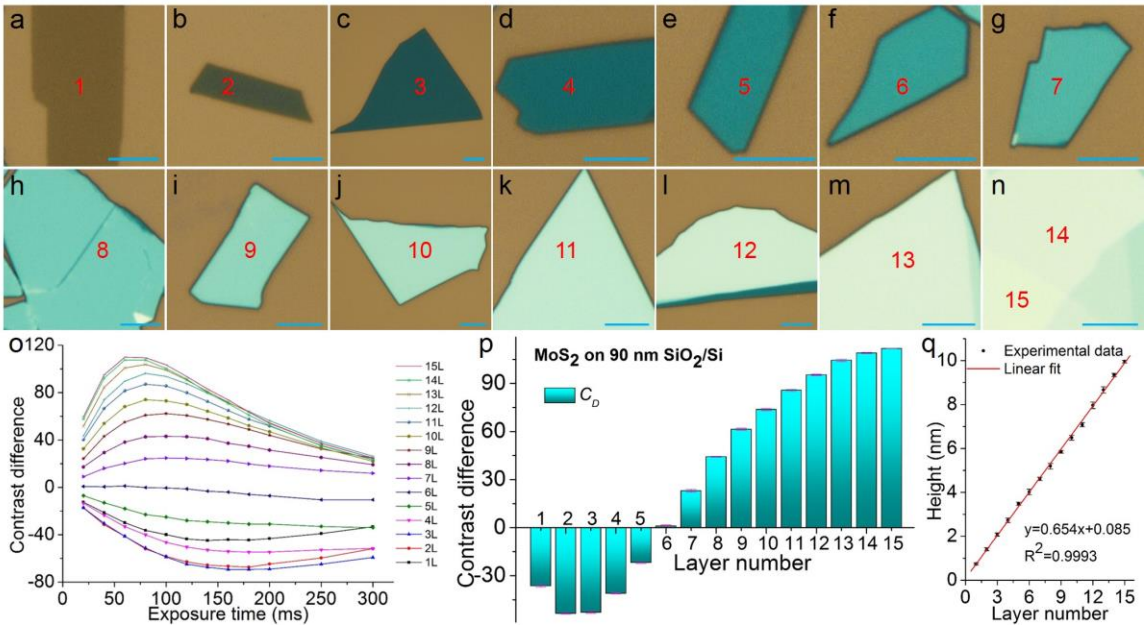

Figure 3. (a-n) Color optical images of 1L-15L MoS_2 nanosheets on 90 nm SiO_2/Si. The scale bar is 5 μm for each image. The digitals shown in (a-n) indicate the layer numbers of corresponding MoS_2 nanosheets. (o) Plot of measured C_D values of 1L-15L MoS_2 nanosheets on 90 nm SiO_2/Si at exposure time of 20, 40, 60, 80, 100, 120, 140, 160, 180, 200, 250 and 300 ms, respectively. (p) Plot of C_D values of 1L-15L MoS_2 on 90 nm SiO_2/Si at exposure time of 80 ms. (q) The thickness of 1L-15L MoS_2 nanosheets measured by AFM.

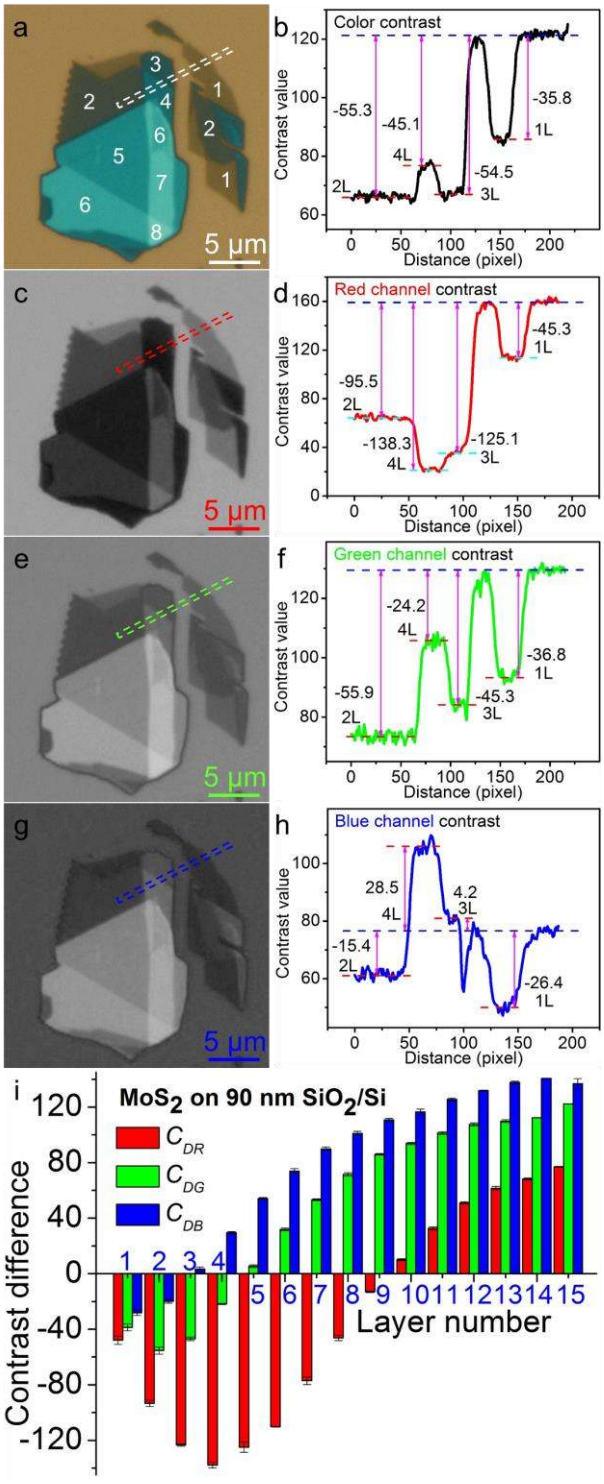

Figure 4. Color optical (a) and grayscale images of the R (c), G (e) and B (g) channels of MoS_2 flake on 90 nm SiO_2/Si. The digitals shown in (a) indicate the layer numbers of corresponding MoS_2 nanosheets. The corresponding contrast profiles of color optical (b)

and grayscale images of the R (d), G (f) and B (h) channels of MoS_2 flake are obtained from the dashed rectangles shown in (a), (c), (e) and (g), respectively. (i) Plot of C_{DR}, C_{DG} and C_{DB} values of 1L-15L MoS_2 nanosheets on 90 nm SiO_2/Si.

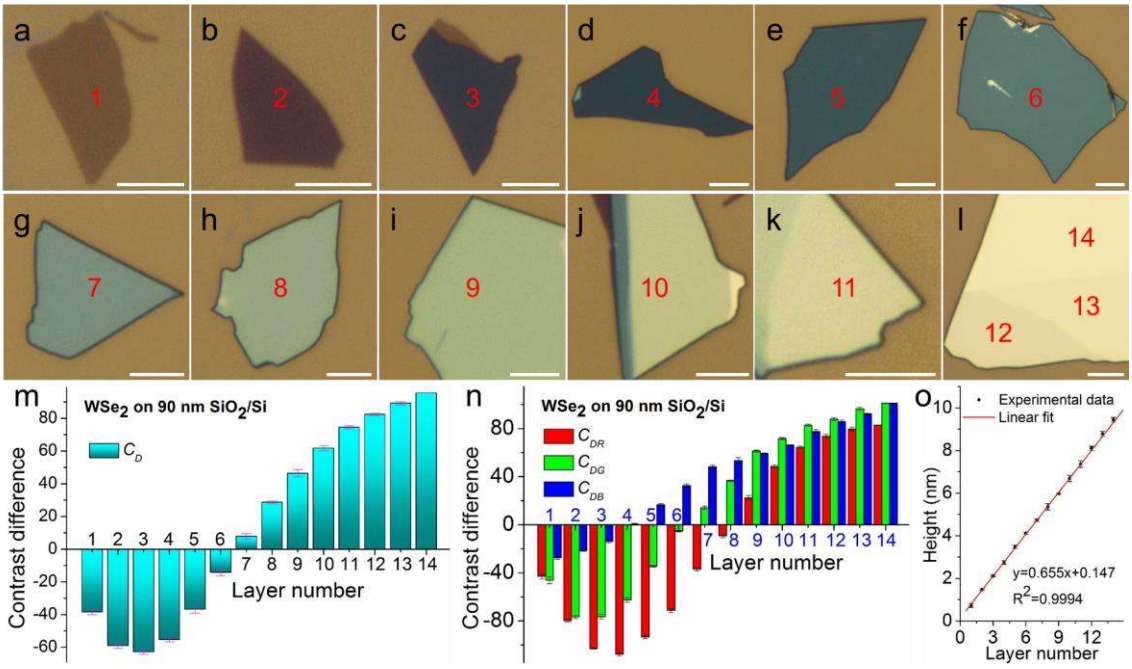

Figure 5. (a-l) Color optical images of 1L-14L WSe_2 nanosheets on 90 nm SiO_2/Si. The scale bars shown in (a-i) are 5 μm. The digitals shown in (a-l) indicate the layer numbers of corresponding WSe_2 nanosheets. (m-n) Plots of (m) C_D and (n) C_{DR}, C_{DG} and C_{DB} values of 1L-14L WSe_2 nanosheets on 90 nm SiO_2/Si at the exposure time of 80 ms. (o) The thickness of 1L-14L WSe_2 nanosheets measured by AFM.

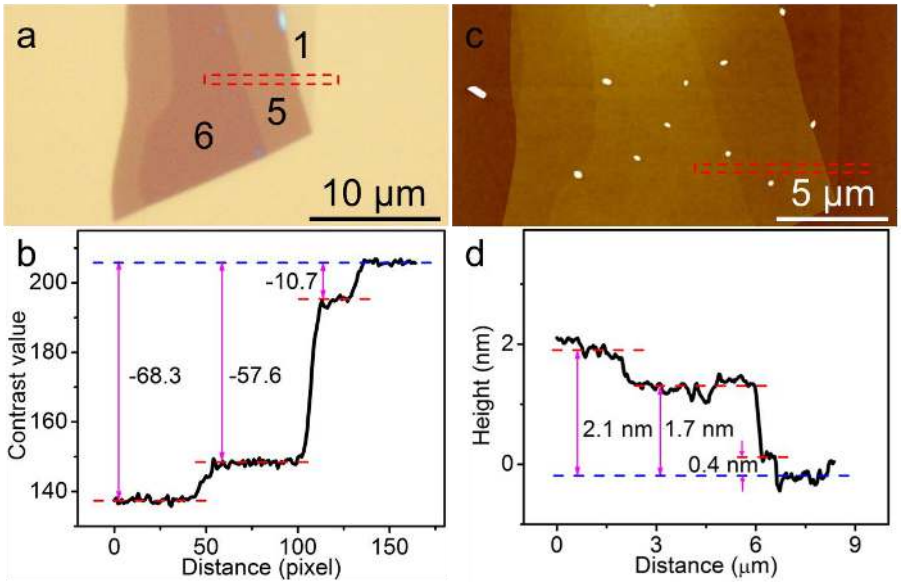

Figure 6. Color optical (a) and AFM height (c) images of graphene flake on 90 nm SiO_2/Si. The corresponding contrast difference (b) and height (d) profiles are obtained from the dashed rectangles shown in (a) and (c), respectively. The digitals shown in (a) indicate the layer numbers of corresponding graphene nanosheets.

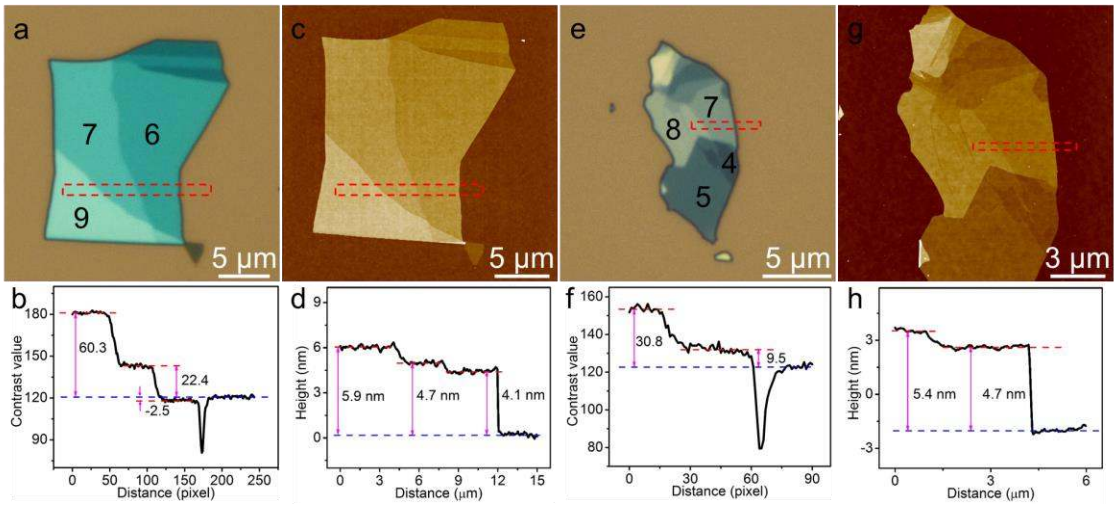

Figure 7. Color optical images of MoS_2 (a) and WSe_2 (e) nanosheets on 90 nm SiO_2/Si and the corresponding contrast profiles (b and f) obtained from the dashed rectangles in (a) and (e), respectively. AFM height images of MoS_2 (c) and WSe_2 (g) nanosheets on 90 nm SiO_2/Si, and the corresponding height profiles (d and h) obtained from the dashed rectangles in (c) and (g), respectively. The digitals shown in (a) and (e) indicate the layer numbers of corresponding MoS_2 and WSe_2 nanosheets, respectively.

Table 1. **The transition thickness of 2D nanosheets with minimum positive optical contrast difference on 90 and 300 nm SiO_2/Si.**

	90 nm SiO_2/Si				300 nm SiO_2/Si			
	C_D	C_{DR}	C_{DG}	C_{DB}	C_D	C_{DR}	C_{DG}	C_{DB}
Graphene	43L < *Tc* < 52L*	54L < *Tc**	43L < *Tc* < 52L*	30L < *Tc* < 37L*	46L < *Tc* < 51L*		~ 46L*	
MoS_2	6L	10L	5L	3L	8L	16L	4L	1L
WSe_2	7L	9L	7L	4L	8L	14L	5L	1L
TaS_2	27L	22L	25L	3L				

*see Figures S12-S13 in Supplementary Information for the detailed information.

Supporting Information

Rapid and reliable thickness identification of two-dimensional nanosheets using optical microscopy

Hai Li,[1,†] Jumiati Wu,[1,†] Xiao Huang,[1] Gang Lu,[1] Jian Yang,[1] Xin Lu,[2] Qihua Xiong,[2] Hua Zhang[1,]*

[1]School of Materials Science and Engineering, Nanyang Technological University, 50 Nanyang Avenue, Singapore 639798, Singapore

[2]Division of Physics and Applied Physics, School of Physical and Mathematical Sciences, Nanyang Technological University, 21 Nanyang Link, Singapore 637371, Singapore

*To whom correspondence should be addressed.

Phone: +65-6790-5175. Fax: +65-6790-9081

E-mail: hzhang@ntu.edu.sg

Website: http://www.ntu.edu.sg/home/hzhang/

[†]These authors contributed equally to this work.

1. Raman spectra of graphene nanosheets on 90 and 300 nm SiO_2/Si.

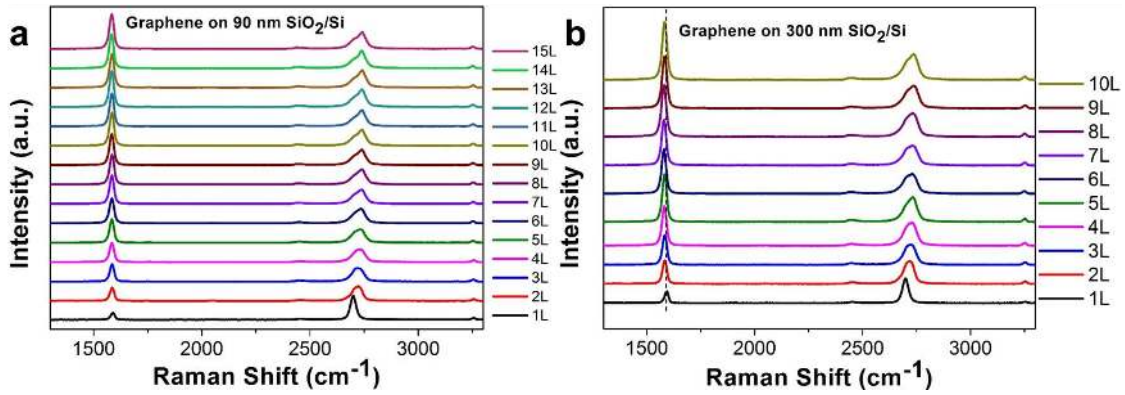

Figure S1. Raman spectra of (a) single- to quindecuple-layer (1L-15L) graphene nanosheets on 90 nm SiO_2/Si, and (b) 1L to decuple-layer (10L) graphene nanosheets on 300 nm SiO_2/Si in the range of 1300-3300 cm^{-1}.

2. Optical identification of 1L-15L graphene nanosheets on 90 nm SiO_2/Si by using C_{DR}, C_{DG} and C_{DB} values.

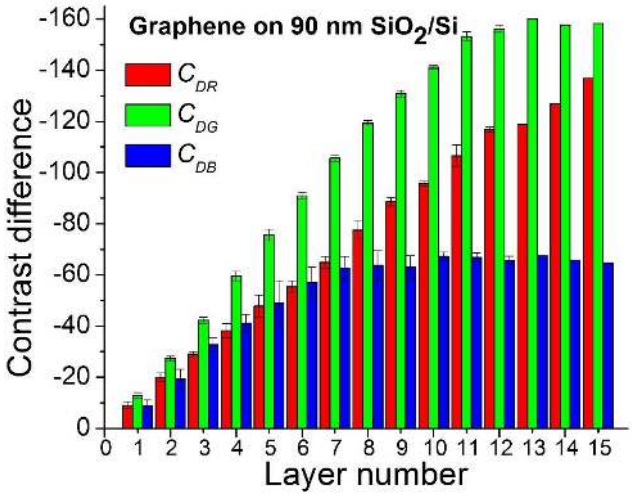

Figure S2. Plot of C_{DR}, C_{DG} and C_{DB} values vs. layer number of 1L-15L graphene nanosheets on 90 nm SiO_2/Si. The original color optical images were taken at exposure

time of 200 ms.

In Figure S2, it can be seen that the C_{DG} values of 1L to undecuple-layer (11L) graphene nanosheets decrease almost linearly with thickness and thus can be used for the thickness identification of graphene. However, for the thicker graphene nanosheets, i.e. tredecuple-layer (13L) to 15L, the C_{DR} values are more suitable for the graphene thickness identification. In addition, the C_{DB} values are distinguishable for 1L to triple-layer (3L) graphene, but show less difference from quadruple-layer (4L) to 15L nanosheets (considering the error bars) and thus are not suitable for thickness identification of 4L-15L graphene.

3. Optical identification of single- to tredecuple-layer (1L-13L) graphene nanosheets on 300 nm SiO_2/Si

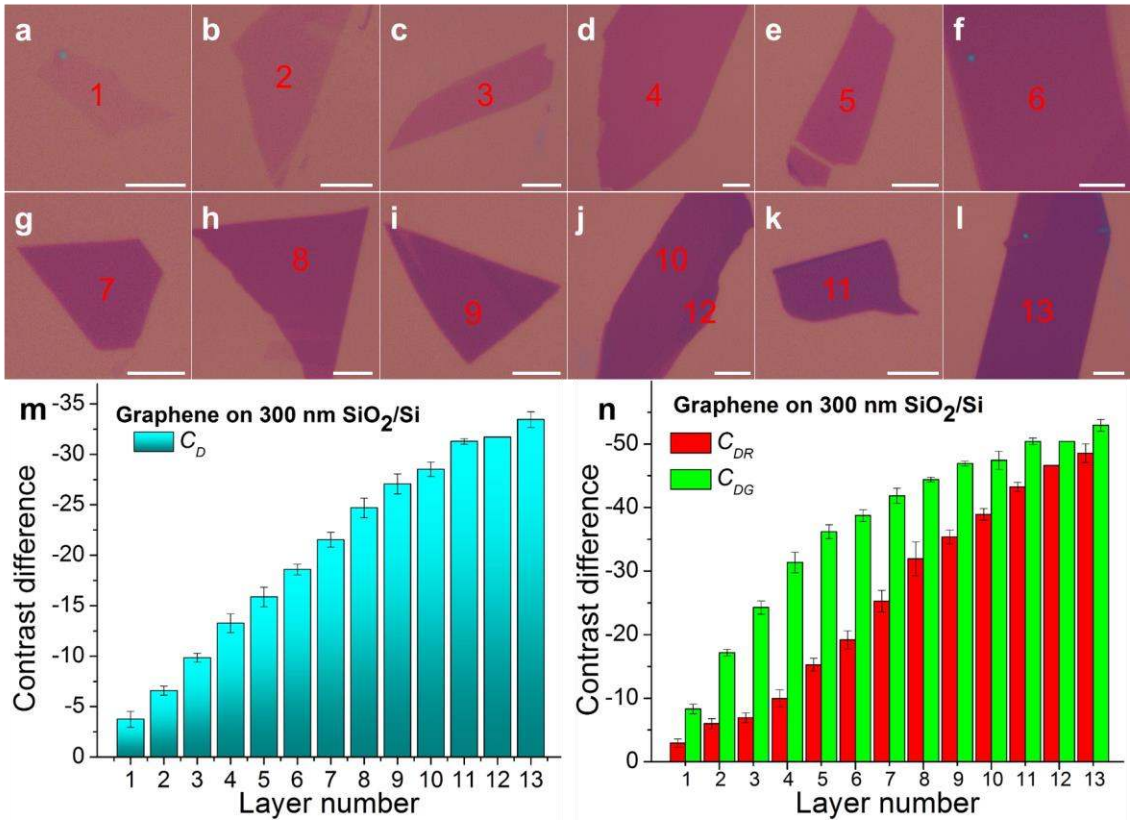

Figure S3. (a-l) Color optical images of 1L-13L graphene nanosheets on 300 nm SiO_2/Si taken at the exposure time of 50 ms. The scale bars shown in (a-l) are 5 μm. The digitals shown in (a-l) indicate the layer numbers of the corresponding graphene nanosheets. (m-n) Plots of (m) C_D values and (n) C_{DR} and C_{DG} values of 1L-13L graphene nanosheets on 300 nm SiO_2/Si.

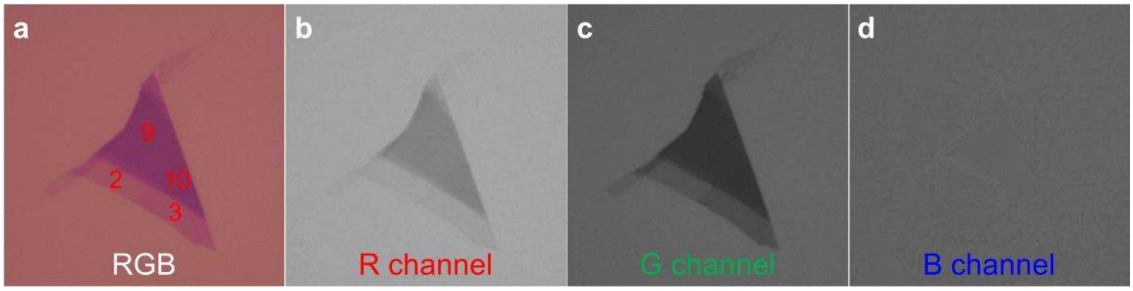

Figure S4. (a) Color optical and (b-d) grayscale images of R, G and B channels of a graphene flake on 300 nm SiO_2/Si. It is difficult to distinguish the graphene flake and substrate in the grayscale image of B channel shown in (d). The digitals shown in (a) indicate the layer numbers of the corresponding graphene nanosheets.

By using 300 nm SiO_2/Si, the C_D values can be used to rapidly and reliably identify the graphene nanosheets from 1L to octuple-layer (8L) (Figure S3m), while the C_{DR} values are suitable for identification of 5L-13L graphene nanosheets (Figure S3n). The C_{DG} values are also suitable for identification of 1L-5L graphene nanosheets (Figure S3n). However, the grayscale image of the B channel of a graphene nanosheet on 300 nm SiO_2/Si does not show obvious contrast between graphene and the substrate, thus the C_{DB} values cannot be used for the identification of graphene thickness (Figure S4d). Therefore, 1L-13L graphene nanosheets on 300 nm SiO_2/Si can be readily identified using the C_D values in combination with the C_{DR} and C_{DG} values.

4. Low-frequency and normal Raman spectra of 1L-15L MoS_2 nanosheets.

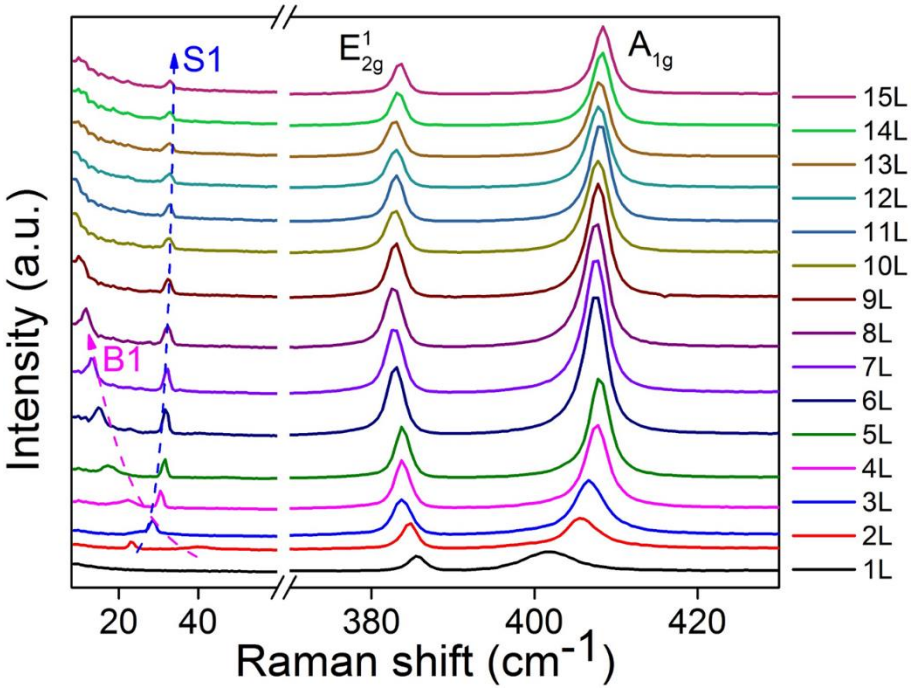

Figure S5. Raman spectra of 1L-15L MoS_2 nanosheets in the range of 8-430 cm^{-1}. Dashed curves are guides for the eyes. S1 and B1 represent the shear and layer breathing (LB) modes, respectively. A_{1g} peaks can be used to identify 1L-4L MoS_2 nanosheets. However, the dependency of A_{1g} peak position on the layer number becomes less obvious for 5L and thicker nanosheets. In addition, the LB mode (B1) peaks can be used to differentiate 1L to nonuple-layer (9L) MoS_2 nanosheets. Note that B1 peaks of 10L-15L nanosheets are out of the detection range of our instrument.

5. Optical identification of 1L-15L MoS_2 nanosheets on 300 nm SiO_2/Si.

1L-15L MoS_2 nanosheets on 300 nm SiO_2/Si can also be identified by measuring the C_D value in combination with the C_{DR}, C_{DG} and C_{DB} values (Figure S6). The C_D values can be used to rapidly and reliably identify septuple-layer (7L) to 15L MoS_2 nanosheets, but are less distinguishable among 1L-6L nanosheets (Figure S6n). In contrast to MoS_2 nanosheets on 90 nm SiO_2/Si (Figure 2 in the main text), the transition of C_D occurs between 7L and 8L MoS_2 nanosheets on 300 nm SiO_2/Si, where 7L MoS_2 gives a negative C_D (-4.4 ± 0.2) and 8L MoS_2 gives a positive C_D (4.7 ± 0.3). The transition of C_D can be used as a mark to quickly determine an MoS_2 nanosheet thicker or thinner than 8L on 300 nm SiO_2/Si. Meanwhile, the C_{DR}, C_{DG} and C_{DB} values are used to identify 1L-6L MoS_2 nanosheets, which are difficult to be distinguished by the measurement of C_D. For example, 1L-3L MoS_2 nanosheets can be differentiated by reading the C_{DR} values (Figure S6o and Table S2), whereas 4L-6L MoS_2 can be distinguished based on C_{DG} values (Figure S6o and Table S2). The T_C of C_{DG} is 4L MoS_2 nanosheet (6.0 ± 1.3), that is, the C_{DG} values of 1L-3L MoS_2 nanosheets are negative while those of 4L-6L MoS_2 nanosheets are positive (See Table S2 for detailed information). The highest absolute value of C_{DR} was found at 6L MoS_2 nanosheet. After that, the absolute C_{DR} values of 7L-15L MoS_2 nanosheets decrease linearly with the thickness. Therefore, 1L-15L MoS_2 nanosheets on 300 nm SiO_2/Si can be readily identified using the C_D values in combination with the C_{DR} and C_{DG} values.

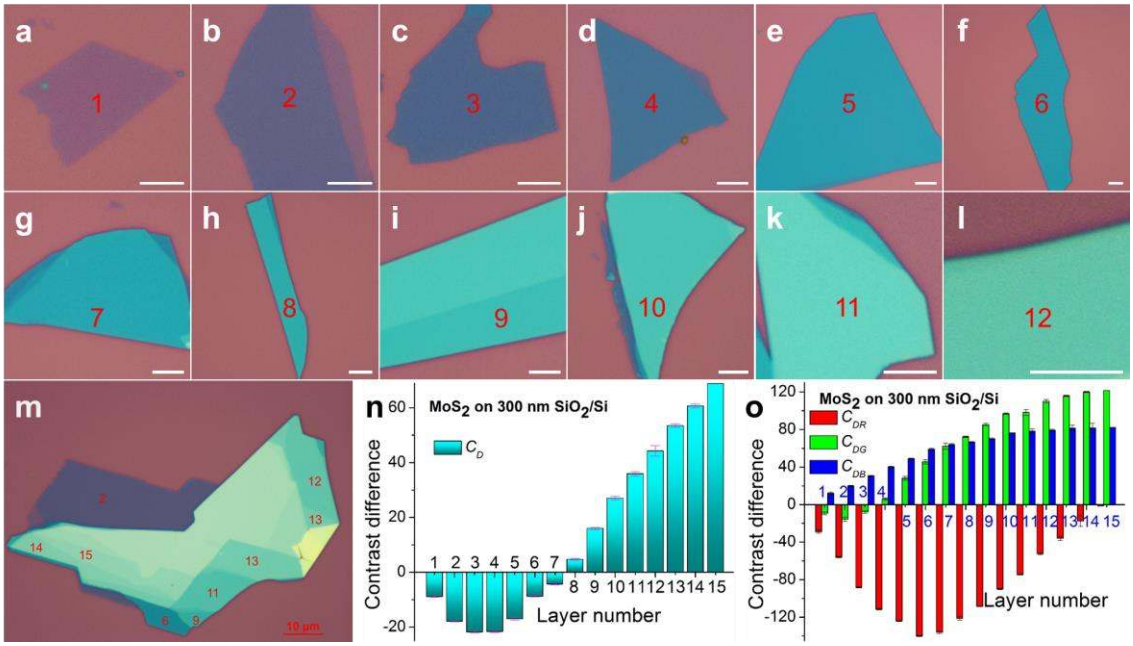

Figure S6. (a-m) Color optical images of 1L-15L MoS_2 on 300 nm SiO_2/Si taken at 50 ms. The scale bars are 5 μm for images a-l and 10 μm for image m, respectively. The digitals shown in (a-m) indicate the layer numbers of the corresponding MoS_2 nanosheets. (n-o) Plots of (n) C_D values and (o) C_{DR}, C_{DG} and C_{DB} values of 1L-15L MoS_2 nanosheets on 300 nm SiO_2/Si.

6. Low-frequency Raman spectra of 1L to quattuordecuple-layer (14L) WSe_2 nanosheets.

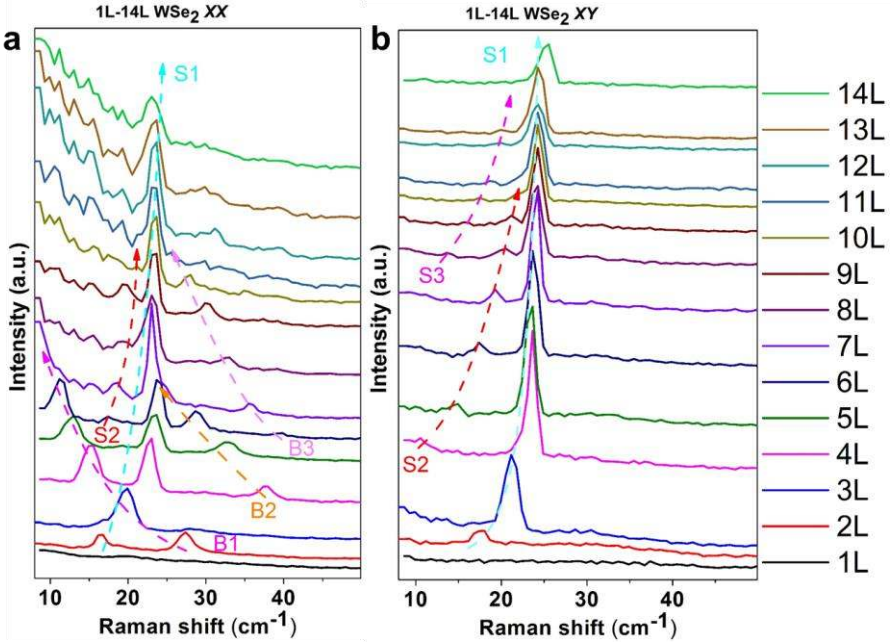

Figure S7. Raman spectra of 1L−14L WSe_2 nanosheets in the range of 8-50 cm^{-1} measured under *XX* (a) and *XY* (b) polarizations, respectively. Dashed curves in (a-b) are guides for the eyes. S1-S3 and B1-B3 represent the shear and layer breathing (LB) modes, respectively. The peaks of shear and LB modes can be used to identify 1L-14L WSe_2 nanosheets. It is clear that B1, B2 and B3 peaks are red-shifted for 2L-6L, 4L-7L and 6L-11L, respectively. S1 peak is blue-shifted from 2L to 4L WSe_2 but its position becomes less affected by layer number for nanosheets thicker than 4L. On the other hand, the blue-shift of S2 and S3 peaks has been observed for 4L-10L and 8L-13L WSe_2, respectively. The low-frequency Raman spectra of 1L-14L WSe_2 nanosheets have been used to confirm that the optical identification result (Figure 5 in the main text) is correct.

7. Optical identification of 1L-14L WSe_2 nanosheets on 300 nm SiO_2/Si.

For the 1L-14L WSe_2 nanosheets on 300 nm SiO_2/Si (Figure S7a-m), the T_C of C_D is 8L (Table 1 and Table S3) and the C_D values of 8L-14L WSe_2 can be used to rapidly and reliably distinguish them (Figure S8n). As for 1L-7L WSe_2 nanosheets, the C_{DR}, C_{DG} and C_{DB} values are used to determine their thicknesses (Table S3 and Figure S8o). Therefore, 1L-14L WSe_2 nanosheets on 300 nm SiO_2/Si can be readily identified using the C_D values in combination with the C_{DR} and C_{DG} values.

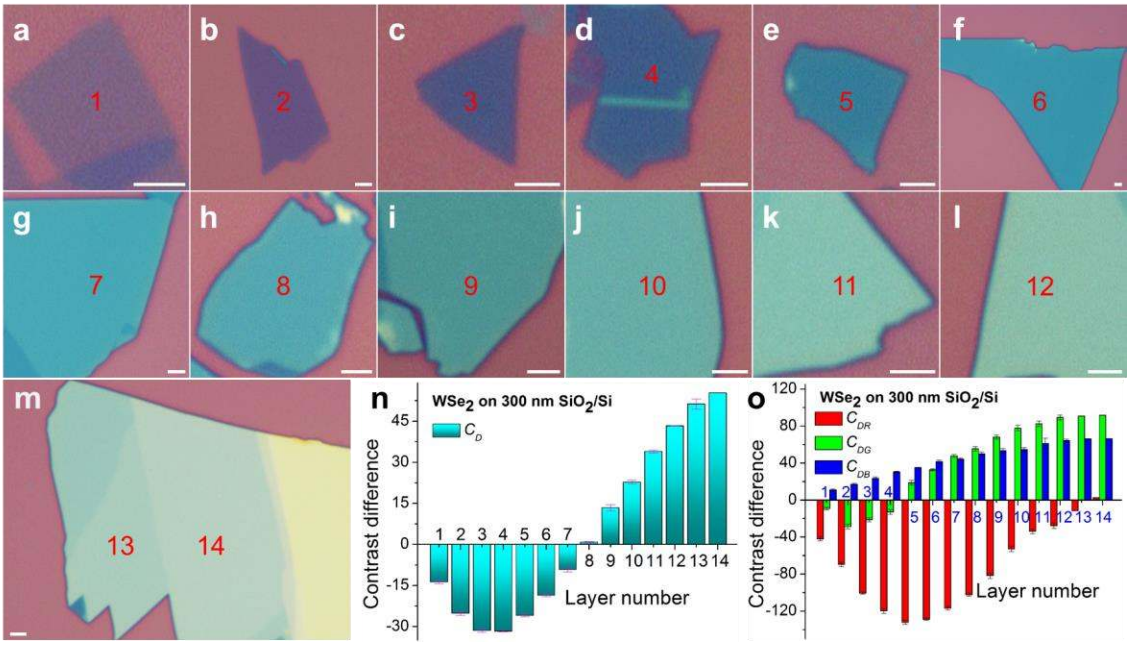

Figure S8. (a-m) Color optical images of 1L-14L WSe_2 on 300 nm SiO_2/Si taken at 50 ms. The scale bars shown in (a-m) are 2 μm. The digitals shown in (a-m) indicate the layer numbers of the corresponding WSe_2 nanosheets. (n-o) Plots of (n) C_D values and (o) C_{DR}, C_{DG} and C_{DB} values of 1L-14L WSe_2 nanosheets on 300 nm SiO_2/Si.

8. Optical identification of 2L to octoviguple-layer (28L) and duotriguple-layer (32L) TaS_2 nanosheets on 90 nm SiO_2/Si.

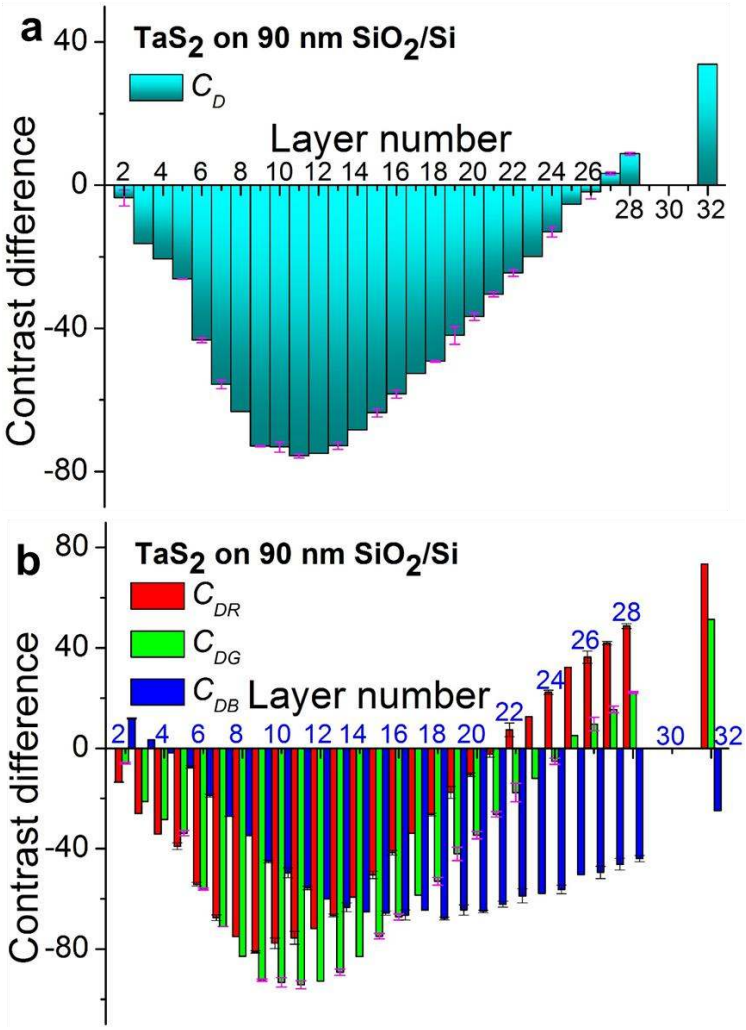

Figure S9. Plots of (a) C_D values and (b) C_{DR}, C_{DG} and C_{DB} values of 2L-28L and 32L TaS_2 nanosheets on 90 nm SiO_2/Si. Original color images were taken at the exposure time of 80 ms.

As shown in Figure S9a, the C_D values of 2L-8L, 15L-28L and 32L TaS_2 nanosheets are discrete enough for reliable identification (Table S4). The 9L-14L TaS_2 nanosheets can be identified by the C_{DR}, C_{DG} and C_{DB} values (Figure S9b). The *Tc* of C_{DR} and C_{DG} is 22L and 25L (Table 1 and Table S4), respectively. Interestingly, the C_{DB} values of 2L-3L TaS_2 nanosheets are positive, and show two *Tc* values with one at 3L and another one probably

larger than 32L. Therefore, the combination of C_D, C_{DR}, C_{DG} and C_{DB} values enables the easy and reliable identification of 2L-28L and 32L TaS_2 nanosheets on 90 nm SiO_2/Si.

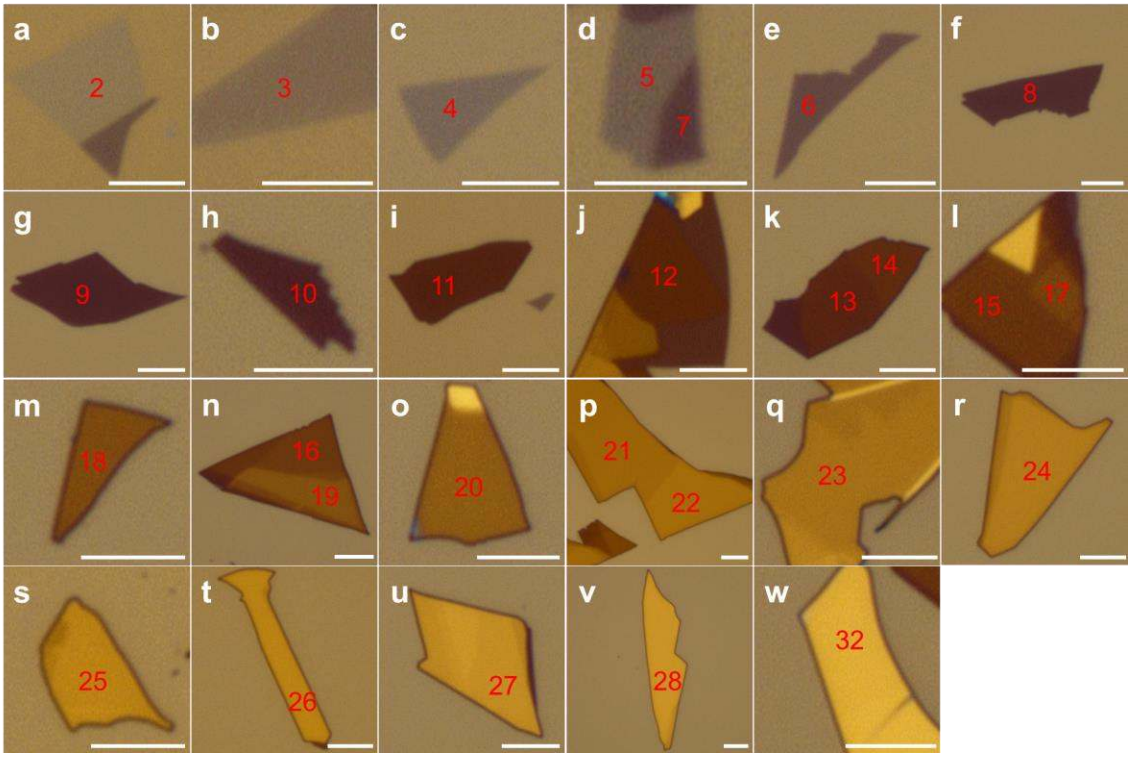

Figure S10. (a-w) Color optical images of 1L-28L and 32L TaS_2 nanosheets on 90 nm SiO_2/Si. The scale bars are 5 μm. The digitals shown in (a-w) indicate the layer numbers of the corresponding TaS_2 nanosheets.

9. Adjustment of light intensity and software configuration of our optical microscope.

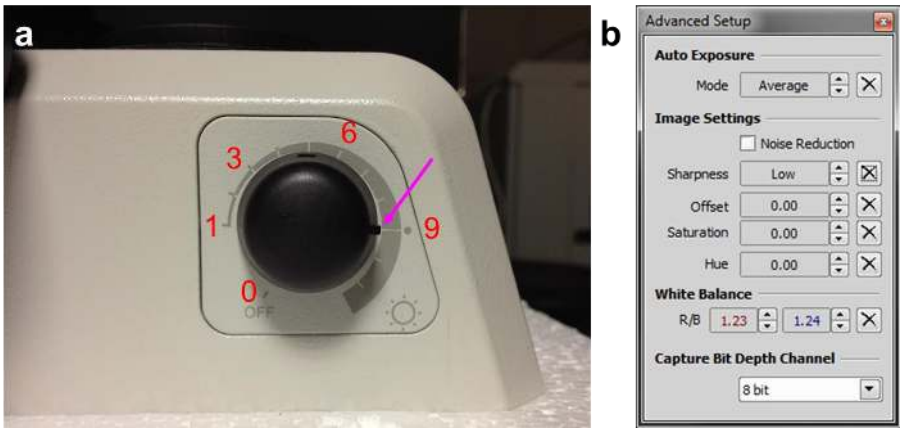

Figure S11. (a) The intensity of light was adjusted by turning the brightness control knob to level 9. (b) Configuration of software for capturing color optical images in the present study.

10. Optical contrast difference (C_D, C_{DR}, C_{DG} and C_{DB}) values of 2D nanosheets.

Table S1. The optical contrast difference (C_D, C_{DR}, C_{DG} and C_{DB}) values of graphene nanosheets with different layer numbers on 90 and 300 nm SiO_2/Si. Optical images of graphene nanosheets on 90 and 300 nm SiO_2/Si were taken at the exposure time of 200 and 50 ms, respectively.

	90 nm SiO_2/Si								**300 nm SiO_2/Si**					
	C_D		C_{DR}		C_{DG}		C_{DB}		C_D		C_{DR}		C_{DG}	
	Mean value	SD	Mean value	SD	Mean value	SD	Mean value	SD	Mean value	SD	Mean value	SD	Mean value	SD
1L	-10.4	0.5	-9.0	1.4	-12.8	1.1	-8.8	2.4	-3.7	0.8	-2.9	0.7	-8.3	0.8
2L	-22.5	0.5	-20.0	1.7	-27.4	0.9	-19.4	3.8	-6.6	0.5	-6.0	0.8	-17.2	0.5
3L	-34.3	0.8	-29.1	1.0	-42.3	1.2	-32.7	2.6	-9.8	0.4	-6.9	0.8	-24.3	1.0
4L	-46.3	0.7	-38.2	2.8	-59.6	1.8	-41.1	3.4	-13.3	0.9	-10.0	1.4	-31.4	1.6
5L	-57.2	0.7	-47.8	4.4	-75.6	2.2	-48.9	9.0	-15.9	1.0	-15.3	1.0	-36.2	1.1
6L	-67.9	0.8	-55.4	2.3	-91.0	1.1	-57.1	5.8	-18.6	0.5	-19.2	1.4	-38.7	0.9
7L	-77.2	0.4	-64.9	2.4	-105.6	1.1	-62.8	4.4	-21.5	0.7	-25.3	1.7	-41.8	1.2
8L	-86.4	0.5	-77.5	3.6	-119.4	0.8	-63.7	5.9	-24.7	1.0	-31.9	2.7	-44.4	0.4
9L	-93.2	1.5	-88.6	1.6	-130.8	1.3	-63.1	4.4	-27.1	1.0	-35.4	1.1	-46.9	0.4
10L	-100.6	0.4	-95.6	0.9	-141.2	0.7	-67.3	1.5	-28.5	0.7	-38.9	0.9	-47.4	1.4
11L	-107.6	0.5	-106.6	4.2	-153.1	1.9	-66.8	1.8	-31.3	0.3	-43.3	0.7	-50.4	0.5
12L	-111.1	1.0	-116.8	0.9	-156.1	1.3	-65.8	1.6	-31.7	0	-46.6	0	-50.4	0
13L	-116.0	0.7	-118.8	0	-160.0	0	-67.5	0	-33.5	0.8	-48.6	1.5	-53.0	0.9
14L	-117.3	0.3	-127	0	-157.7	0	-65.8	0						
15L	-119.7	0	-136.8	0	-158.3	0	-64.7	0						

Table S2. The optical contrast difference (C_D, C_{DR}, C_{DG} and C_{DB}) values of MoS_2 nanosheets with different layer numbers on 90 and 300 nm SiO_2/Si. Optical images of MoS_2 nanosheets on 90 and 300 nm SiO_2/Si were taken at the exposure time of 80 and 50 ms, respectively.

	90 nm SiO_2/Si								**300 nm SiO_2/Si**							
	C_D		C_{DR}		C_{DG}		C_{DB}		C_D		C_{DR}		C_{DG}		C_{DB}	
	Mean value	SD	Mean value	SD	Mean value	SD	Mean value	SD	Mean value	SD	Mean value	SD	Mean value	SD	Mean value	SD
1L	-36.3	0.8	-47.9	2.9	-38.7	2.4	-28.1	2.0	-8.9	0.2	-28.8	1.8	-9.3	1.5	12.1	1.0
2L	-53.6	0.5	-93.3	2.3	-55.4	2.6	-19.9	1.3	-17.9	0.2	-55.9	0.8	-15.7	2.2	19.7	0.9
3L	-52.9	0.6	-123.4	0.8	-47.0	1.3	3.4	1.4	-21.8	0.3	-88.1	0.5	-7.9	1.6	30.5	0.7
4L	-41.1	0.3	-137.9	2.2	-21.8	0.5	29.5	0.9	-21.7	0.4	-111.3	0.9	6.0	1.3	40.1	0.6
5L	-21.8	0.5	-125.0	3.7	5.4	0.9	54.1	0.8	-17.0	0.5	-124.0	0.4	28.1	2.1	49.0	0.6
6L	1.0	0.7	-110.2	0.3	31.8	1.0	73.8	1.9	-8.8	0.2	-139.9	0.6	45.7	2.5	58.9	1.1
7L	23.0	0.9	-77.1	2.7	53.3	0.7	89.9	1.2	-4.4	0.2	-136.1	1.3	62.3	3.5	64.0	0.9
8L	44.3	0.3	-46.3	2.0	71.5	1.3	101.0	1.5	4.7	0.3	-121.1	2.0	72.2	0.7	66.5	0.5
9L	61.4	0.7	-13.0	0.6	85.9	0.6	110.7	1.2	16.0	0.4	-108.4	0.3	85.3	1.3	70.1	0.8
10L	73.8	0.7	10.1	0.6	93.8	0.8	116.5	2.0	27.0	0.6	-89.8	0.7	96.8	0.9	76.4	0.3
11L	85.7	0.7	32.6	1.0	101.4	1.0	125.6	1.0	35.9	0.8	-74.6	0.4	98.2	3.3	78.2	2.4
12L	95.4	0.5	51.0	0.8	107.5	1.0	131.9	0.3	44.3	1.9	-52.5	0.9	110.0	2.0	79.2	0.9
13L	104.5	0.8	61.6	1.2	109.8	1.0	137.8	0.9	53.4	0.6	-35.9	2.1	115.9	0.5	81.5	3.1
14L	109.0	0.3	68.2	0.7	112.3	0.1	140.6	0.1	60.7	0.7	-17.4	5.8	119.9	0.7	81.6	5.0
15L	111.80063	0.1	77.0	0.3	122.3	0.1	136.8	3.7	68.8	0	-1.3	0	121.5	0	82.1	0

Table S3. The optical contrast difference (C_D, C_{DR}, C_{DG} and C_{DB}) values of WSe_2 nanosheets with different layer numbers on 90 and 300 nm SiO_2/Si. Optical images of WSe_2 nanosheets on 90 and 300 nm SiO_2/Si were taken at the exposure time of 80 and 50 ms, respectively.

	90 nm SiO_2/Si								**300 nm SiO_2/Si**							
	C_D		C_{DR}		C_{DG}		C_{DB}		C_D		C_{DR}		C_{DG}		C_{DB}	
	Mean value	SD	Mean value	SD	Mean value	SD	Mean value	SD	Mean value	SD	Mean value	SD	Mean value	SD	Mean value	SD
1L	-38.4	1.7	-43.0	2.1	-46.3	2.7	-27.6	1.4	-13.7	0.6	-41.9	2.4	-9.3	1.3	11.0329	1.1
2L	-59.2	1.4	-80.0	0.9	-76.8	1.4	-21.6	0.5	-25.2	0.7	-69.5	2.4	-28.8	2.6	17.1861	1.0
3L	-62.9	1.5	-103.0	0.4	-76.5	1.9	-13.9	1.2	-31.5	0.6	-100.7	1.2	-21.2	2.3	23.55704	1.4
4L	-55.3	1.4	-107.9	1.4	-62.7	1.9	0.3	0.8	-31.8	0.2	-119.7	2.8	-12.9	2.6	30.29348	0.8
5L	-36.8	2.4	-93.6	1.2	-34.7	0.7	16.7	0.9	-26.0	0.6	-132.0	2.2	18.6	2.6	35.01708	0.4
6L	-14.2	2.1	-71.3	1.8	-5.5	0.6	32.4	1.5	-18.6	0.6	-128.8	1.3	32.8	1.2	41.65274	1.6
7L	7.8	1.7	-37.0	1.3	14.1	1.3	48.1	1.3	-9.2	0.9	-117.0	2.1	47.7	1.5	44.15263	1.1
8L	28.6	0.9	-9.2	1.5	36.6	0.4	53.2	2.7	0.8	0.2	-102.3	1.7	55.3	2.5	49.98872	1.8
9L	46.4	2.1	22.3	2.0	61.2	0.9	59.1	0.5	13.4	1.2	-81.7	3.1	68.0	2.2	53.38465	2.2
10L	61.8	1.5	48.4	1.3	71.7	0.9	66.2	0.3	22.7	0.7	-52.9	2.9	77.6	2.9	54.51789	2.1
11L	74.5	0.9	64.4	1.0	82.7	0.9	77.4	1.5	33.9	0.5	-33.9	2.6	82.5	3.0	61.04936	5.7
12L	82.4	0.9	73.6	1.3	87.7	1.1	85.8	1.1	43.3	0.1	-27.7	2.9	89.3	2.7	64.37087	1.4
13L	89.3	1.0	79.6	1.5	96.5	1.3	92.2	0.5	51.3	1.8	-11.4	0	90.7	0	66.02392	0
14L	95.5	0	82.9	0	101.2	0	101.0	0	55.3	0	2.4	0	91.7	0	66.27921	0

Table S4. The optical contrast difference (C_D, C_{DR}, C_{DG} and C_{DB}) values of TaS_2 nanosheets with different layer numbers on 90 nm SiO_2/Si. Optical images were taken at the exposure time of 80 ms.

	90 nm SiO_2/Si							
	C_D		C_{DR}		C_{DG}		C_{DB}	
	Mean value	SD	Mean value	SD	Mean value	SD	Mean value	SD
2L	-3.6	2.2	-13.5	0.1	-6.0	0.3	11.9	0.2
3L	-12.1	1.8	-18.6	0.2	-16.2	1.5	0.4	1.6
4L	-18.5	3.0	-36.1	2.8	-24.8	5.1	-4.5	3.7
5L	-26.2	0	-39.9	0	-34.5	0	-7.7	0
6L	-43.3	0.7	-54.1	0.7	-56.0	0.4	-18.9	0.6
7L	-55.7	1.2	-67.4	1.1	-71.0	0.1	-27.1	0.2
8L	-63.3	0	-74.9	0	-82.8	0	-34.7	0
9L	-72.9	0.1	-81.1	0.5	-92.3	0.5	-45.1	0.6
10L	-73.2	1.4	-77.6	2.1	-93.2	1.8	-49.6	2.0
11L	-75.7	0.5	-75.5	2.5	-94.2	1.6	-55.6	0.7
12L	-75.0	0	-71.8	0	-92.7	0	-60.0	0
13L	-72.8	1.0	-66.5	0.6	-89.2	1.2	-63.3	1.8
14L	-68.4	0	-59.3	0	-82.9	0	-65.1	0
15L	-63.6	1.1	-50.4	1.5	-74.8	1.1	-65.7	0.8
16L	-58.4	1.1	-41.6	0.9	-67.1	1.2	-66.4	1.9
17L	-52.7	0	-33.8	0	-58.5	0	-64.4	0
18L	-49.3	0.2	-26.4	0.6	-52.9	1.5	-67.8	0.5
19L	-42.0	2.5	-17.6	2.4	-42.0	2.6	-64.4	2.1
20L	-36.7	1.1	-10.5	0.7	-34.6	1.5	-65.0	0.5
21L	-30.5	0.7	-2.3	1.2	-26.3	1.1	-62.1	1.2
22L	-24.5	0.9	7.3	2.7	-17.6	3.7	-58.8	2.8
23L	-20.0	0	12.5	0	-12.0	0	-57.7	0
24L	-13.1	1.4	22.3	0.8	-5.2	1.2	-56.2	1.7
25L	-5.3	0	32.2	0	5.0	0	-50.3	0
26L	-1.9	1.9	36.3	2.4	9.7	2.7	-49.4	2.4
27L	3.3	0.4	41.9	0.7	15.5	1.3	-46.1	2.3

28L	8.8	0.4	48.7	1.0	22.2	0.3	-44.0	1.2
32L	33.8	0	73.3	0	51.4	0	-24.9	0

11. Thickness of various 2D nanosheets measured by AFM.

Table S5. Thicknesses of graphene, MoS_2 and WSe_2 nanosheets with different layer numbers measured by AFM.

	Graphene		**MoS_2**		**WSe_2**		**TaS_2**	
	Mean value (nm)	SD	Mean value (nm)	SD	Mean value (nm)	SD	Mean value (nm)	SD
1L	0.4	0.1	0.7	0.1	0.7	0.1		
2L	0.7	0.1	1.4	0.1	1.5	0.1	1.4	0.1
3L	1.0	0.1	2.1	0.1	2.1	0.1	1.9	0.1
4L	1.4	0.1	2.7	0.1	2.8	0.1	2.6	0.1
5L	1.7	0.1	3.5	0.1	3.5	0.1	3.3	0.1
6L	2.0	0.1	4.0	0.1	4.1	0.1	4.0	0.1
7L	2.4	0.1	4.6	0.1	4.7	0.1	4.6	0.1
8L	2.8	0.1	5.2	0.1	5.4	0.1	5.3	0.1
9L	3.1	0.1	5.9	0.1	6.0	0.1	6.0	0.1
10L	3.4	0.1	6.5	0.1	6.7	0.1	6.6	0.1
11L	3.7	0.1	7.1	0.1	7.4	0.2	7.2	0.1
12L	4.1	0.1	8.0	0.1	8.1	0.1	8.0	0.1
13L	4.4	0.1	8.7	0.1	8.8	0.1	8.5	0.1
14L	4.8	0.1	9.3	0.1	9.4	0.1	9.1	0.1
15L	5.2	0.1	10.0	0.1			9.8	0.1
16L							10.5	0.1
17L							10.9	0.1
18L							11.6	0.1
19L							12.3	0.1
20L							12.9	0.1
21L							13.6	0.1
22L							14.2	0.1
23L							14.9	0.1
24L							15.5	0.1
25L							16.1	0.1
26L							16.7	0.1
27L							17.5	0.1
28L							18.1	0.1

32L							20.7	0.2

12. The thickness of graphene nanosheets with minimum positive optical contrast difference on 90 and 300 nm SiO_2/Si.

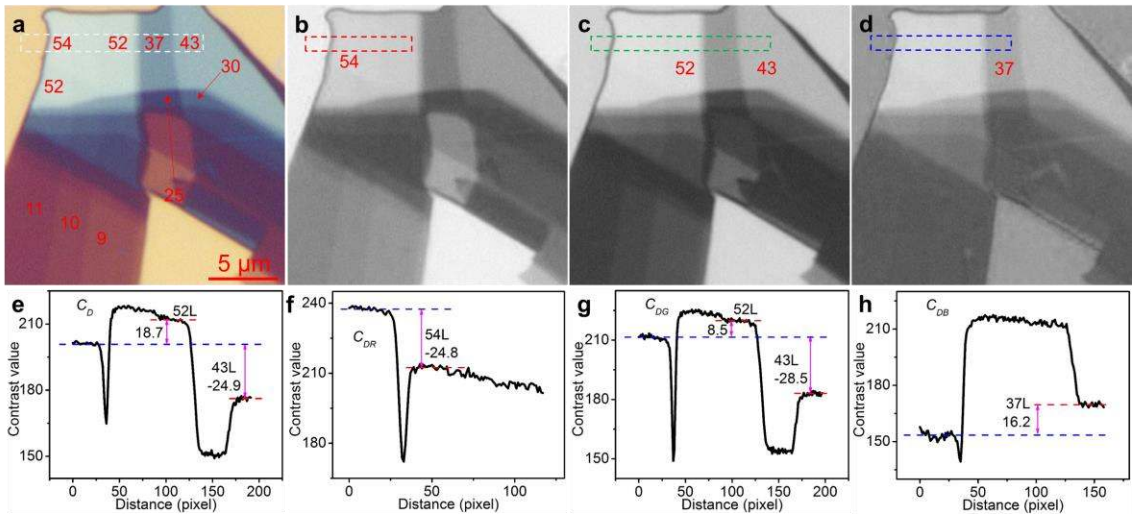

Figure S12. Color optical images (a) and grayscale images of R (b), G (c), and B (d) channels of graphene nanosheets on 90 nm SiO_2/Si and the corresponding contrast profiles (e-h) of the dashed rectangles shown in (a-d), respectively. The digitals shown in (a-d) indicate the layer numbers of corresponding graphene nanosheets.

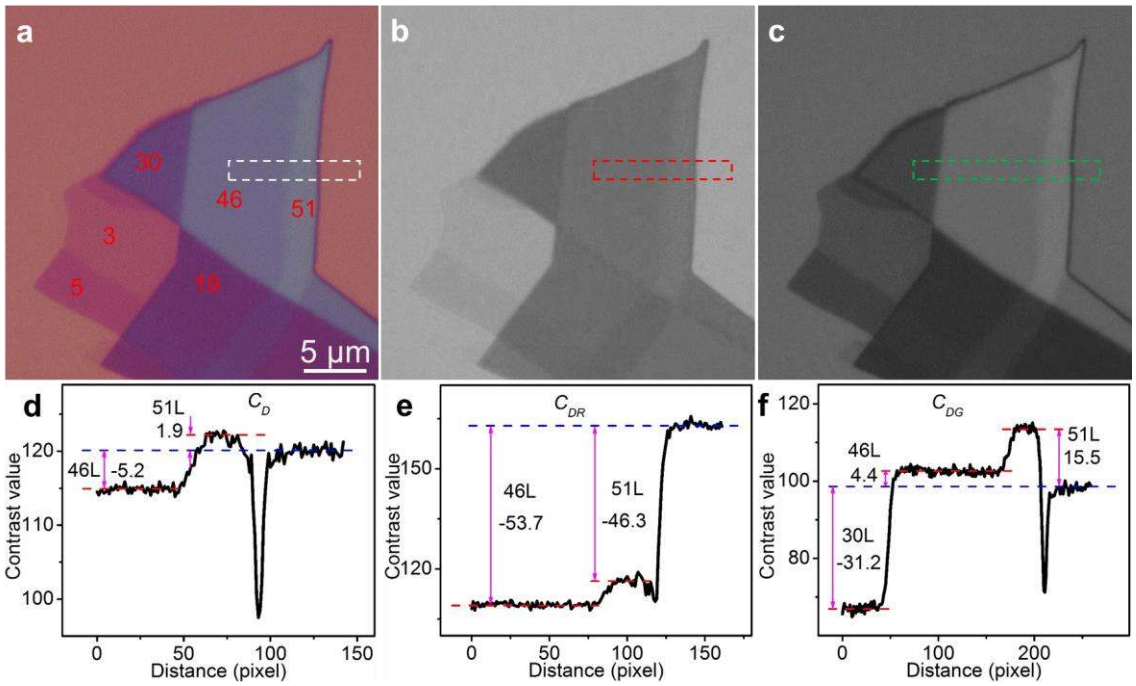

Figure S13. Color optical images (a) and grayscale images of R (b) and G (c) channels of graphene nanosheets on 300 nm SiO_2/Si and the corresponding contrast profiles (d-f) of the dashed rectangles shown in (a-c), respectively. The digitals shown in (a) indicate the layer numbers of corresponding graphene nanosheets.